Spatial Trade with Transportation Markets

Online Appendix

Busra Ariduru* Germán Pupato†

April 28, 2026

Online Appendix — Table of Contents

*Department of Economics, Toronto Metropolitan University; eariduru@torontomu.ca
†Department of Economics, Toronto Metropolitan University; gpupato@torontomu.ca

A Theoretical Framework: Derivations and Proofs

This appendix derives the equilibrium equations used in the main text, presents the algorithm used to solve the model, and proves Propositions 1–4. Subsection A.1 derives prices and trade shares (Eaton–Kortum machinery) and the population-mobility condition (Helpman-housing structure). Subsection A.2 contains the derivations that are *specific* to this paper—the transportation demand aggregation, the multinomial-logit selection over destinations, and the Gumbel log-sum free-entry identity—and are presented in full. Subsection A.3 characterizes the Iceberg Limit. Subsection A.4 presents the algorithm we use to compute baseline and counterfactual equilibria. Subsections A.5–A.7 prove Propositions 1–3, and Subsection A.8 proves Proposition 4 in the symmetric setting introduced in the same subsection. Subsection A.9 reports the parameter values used in the symmetric numerical example of Section 3.3.

A.1 Equilibrium Derivations

Prices. For tradable good $j \geq 1$, consumers source each variety from the cheapest location, paying $p_n^j(\omega^j) = \min_i(\varphi_i^j w_i + t_{ni})/z_i^j(\omega^j)$. With $z_i^j(\omega^j)$ drawn from a Fréchet distribution with scale A_i^j and shape θ^j, the origin-i price distribution at destination n is

$$G_{ni}^j(p) = 1 - \exp\big[-A_i^j(\varphi_i^j w_i + t_{ni})^{-\theta^j} p^{\theta^j}\big]. \tag{A.1}$$

Independence of $z_i^j(\omega^j)$ across i gives the destination price distribution

$$G_n^j(p) = 1 - \exp(-\Phi_n^j p^{\theta^j}), \qquad \Phi_n^j = \sum_i A_i^j(\varphi_i^j w_i + t_{ni})^{-\theta^j}. \tag{A.2}$$

Substituting (A.2) into $(P_n^j)^{1-\sigma^j} = \int_0^\infty p^{1-\sigma^j}\, dG_n^j(p)$ and using the gamma-function identity of Eaton and Kortum (2002) yields

$$P_n^j = \Gamma^j\,(\Phi_n^j)^{-1/\theta^j}, \qquad \Gamma^j \equiv \Gamma\Big(\tfrac{\theta^j+1-\sigma^j}{\theta^j}\Big)^{1/(1-\sigma^j)}. \tag{A.3}$$

Trade shares. Consumers in n purchase from origin i whenever its price is the lowest. Standard Eaton–Kortum arithmetic gives

$$\pi_{ni}^{j} = \Pr\Big[p_{ni}^{j}(\omega^{j}) \le \min_{m\neq i} p_{nm}^{j}(\omega^{j})\Big] = \frac{A_i^{j}(\varphi_i^{j} w_i + t_{ni})^{-\theta^{j}}}{\Phi_n^{j}}, \quad j \ge 1, \tag{A.4}$$

i.e., origin i's share of the multilateral resistance denominator Φ_n^{j}.

Income and population mobility. Expenditure on residential land is rebated lump-sum to local residents, so per-worker nominal income satisfies $v_n L_n = w_n L_n + (1-\alpha)\, v_n L_n$, i.e.

$$v_n L_n = w_n L_n / \alpha. \tag{A.5}$$

Combining trade balance with $\alpha X_n = w_n L_n$, land market clearing $r_n H_n = (1-\alpha) v_n L_n$, and the population mobility condition $v_n/(P_n^{\alpha} r_n^{1-\alpha}) = \bar{U}$, we obtain indirect utility in location n:

$$U_n = \frac{w_n^{\alpha} H_n^{1-\alpha}}{\alpha \left(\frac{1-\alpha}{\alpha}\right)^{1-\alpha} L_n^{1-\alpha} P_n^{\alpha}} = \bar{U}. \tag{A.6}$$

Rearranging for L_n and dividing by the U.S. population constraint gives (15) of the main text.

A.2 Transportation Markets: Demand, Supply, and Free Entry

Demand for transportation services. CES demand plus the Leontief technology (4) gives, for each variety,

$$k_{ni}^{j}(\omega^{j}) = X_n^{j} (P_n^{j})^{\sigma^{j}-1} (\varphi_i^{j} w_i + t_{ni})^{-\sigma^{j}}\, z_i^{j}(\omega^{j})^{\sigma^{j}-1}, \qquad j \ge 1, \tag{A.7}$$

where $X_n^{j} = \alpha^{j} X_n$ is expenditure on sector j in n. Aggregating $k_{ni}^{j} = \int_0^1 k_{ni}^{j}(\omega^{j})\, d\omega^{j}$ requires evaluating $\int_0^1 z_i^{j}(\omega^{j})^{\sigma^{j}-1}\, d\omega^{j}$ on the set where i is the lowest-cost supplier to n. This step is specific to our setting: the productivity draws are not independent of the selection event.

By Bayes' rule, the conditional CDF of z_i^{j} given that i is the lowest-cost supplier to n can be derived from the joint distribution of $(z_i^{j},\, p_{ni}^{j} \le \min_{m\neq i} p_{nm}^{j})$. Substituting the Fréchet density and integrating the joint over prices above $(\varphi_i^{j} w_i + t_{ni})/z$ gives

$$\Pr\big[z_i^{j}(\omega^{j}) \le z \;\big|\; i \text{ supplies } n\big] = \exp\big[-\Phi_n^{j} (\varphi_i^{j} w_i + t_{ni})^{\theta^{j}}\, z^{-\theta^{j}}\big]. \tag{A.8}$$

The conditional distribution is again Fréchet, with a scale that depends on i only through the destination aggregate Φ_n^{j}. The moment $\int z^{\sigma^{j}-1}\, dG$ is then evaluated by the same

substitution $u = \Phi_n^j(\varphi_i^j w_i + t_{ni})^{\theta^j} z^{-\theta^j}$ that produced the price index:

$$\int_0^1 z_i^j(\omega^j)^{\sigma^j-1}\, d\omega^j = \pi_{ni}^j\,(\varphi_i^j w_i + t_{ni})^{\sigma^j-1}(\Phi_n^j)^{(\sigma^j-1)/\theta^j}\,\Gamma^{j\,1-\sigma^j}. \tag{A.9}$$

Inserting (A.9) and (A.3) into (A.7), the σ^j-dependent factors cancel and we obtain the demand for transportation services from i to n for good j:

$$k_{ni}^j = \frac{X_n^j\,\pi_{ni}^j}{\varphi_i^j w_i + t_{ni}}. \tag{A.10}$$

Aggregating over sectors gives $k_{ni} = \sum_j k_{ni}^j$; aggregating over destinations gives origin supply $k_i = \sum_n k_{ni}$.

Supply of transportation services. Upon entry, trucker r at origin i chooses destination n to maximise

$$\Pi_{ni}(r) = t_{ni} - w_i c_{ni} + w_i \nu\, \epsilon_{ni}(r), \tag{A.11}$$

with $\epsilon_{ni}(r)$ i.i.d. Gumbel with location $-\bar{\gamma}$ and unit scale. Defining $V_{ni} \equiv t_{ni}/(w_i\nu) - c_{ni}/\nu$ and writing the discrete-choice probability in the standard form,

$$\Pr\big[\, n = \arg\max_h \Pi_{hi}(r)\,\big] = \int_{-\infty}^{\infty} f(\epsilon_{ni}) \prod_{h\neq n} F\big(\epsilon_{ni} + V_{ni} - V_{hi}\big)\, d\epsilon_{ni}. \tag{A.12}$$

With independent Gumbel shocks, the product of CDFs collapses to a single exponential, and with the substitution $u = \epsilon_{ni} + \bar{\gamma}$ followed by $y = u - \lambda$ with $\lambda \equiv \log\sum_h \exp(V_{hi}) - V_{ni}$, the integrand in (A.12) becomes the density of a standard Gumbel and integrates to unity.[1] Therefore

$$\Pr\big[\, n = \arg\max_h \Pi_{hi}(r)\,\big] = \frac{\exp V_{ni}}{\sum_h \exp V_{hi}} = \frac{\exp\!\big(\frac{t_{ni}}{w_i\nu} - \frac{c_{ni}}{\nu}\big)}{\sum_h \exp\!\big(\frac{t_{hi}}{w_i\nu} - \frac{c_{hi}}{\nu}\big)}. \tag{A.13}$$

By the law of large numbers, the trucker share k_{ni}/k_i equals the choice probability (A.13), giving the supply function (9) in the main text.

Free entry condition. Free entry requires that the ex-ante expected profit of a trucker at origin i (inclusive of the entry cost) equals zero:

$$\mathbb{E}(\Pi_i) = \sum_{n=1}^{N} (\Pi_{ni} \mid n \text{ chosen}) \cdot \Pr\big[n = \arg\max_h \Pi_{hi}\big] = w_i f_i. \tag{A.14}$$

[1] This is the standard multinomial-logit derivation. We spell out the algebra because the conditional-expectation identity used in the free-entry derivation below requires the same change of variables.

The conditional expectation $\mathbb{E}[\epsilon_{ni} \mid n \text{ chosen}]$ is the model-specific step. Its derivation uses the conditional CDF of ϵ_{ni} given that destination n maximises profit. Applying Bayes' rule to the integral in (A.12),

$$\Pr\big[\,\epsilon_{ni} \geq \epsilon \mid n \text{ chosen}\big] = 1 - \exp\Big[-\exp\big(-(\epsilon + \bar{\gamma} - \lambda)\big)\Big], \tag{A.15}$$

which is a Gumbel CDF with location $\lambda - \bar{\gamma}$. Therefore $\mathbb{E}[\epsilon_{ni} \mid n \text{ chosen}] = \lambda$, i.e. the destination-specific log-sum net of V_{ni}.[2] Substituting $\mathbb{E}[\epsilon_{ni} \mid n] = \lambda$ into $\Pi_{ni} \mid n$ gives the conditional profit

$$\Pi_{ni} \mid n = t_{ni} - w_i c_{ni} + w_i \nu \lambda. \tag{A.16}$$

Inserting (A.16) and (A.13) into (A.14), using $\sum_n \exp(V_{ni}) / \sum_h \exp(V_{hi}) = 1$, the cross-terms involving V_{ni} cancel pairwise and we obtain

$$\mathbb{E}(\Pi_i) = w_i \nu \log \sum_h \exp\Big(\tfrac{t_{hi}}{w_i \nu} - \tfrac{c_{hi}}{\nu}\Big), \tag{A.17}$$

yielding the free-entry condition (10) of the main text, $f_i = \nu \log \sum_h \exp(V_{hi})$.

A.3 The Iceberg Limit

As $\nu \to 0$, inverting transportation supply (9) under free entry (10) pins down relative transportation prices exogenously. In any active market ($k_{ni} > 0$),

$$\frac{t_{ni}}{w_i} = c_{ni} + f_i. \tag{A.18}$$

Under (A.18), the unit cost in destination n factorises as $\varphi_i^j w_i + t_{ni} = w_i \tau_{ni}^j$, with exogenous iceberg cost

$$\tau_{ni}^j \equiv \varphi_i^j + c_{ni} + f_i. \tag{A.19}$$

[2] The conditional Gumbel identity $\mathbb{E}[\epsilon \mid n \text{ chosen}] = \log \sum_h \exp(V_{hi}) - V_{ni}$ is classical in discrete choice. We record it here because it converts the free-entry condition into the closed-form log-sum expression (A.17).

Substituting into (5)–(15) of the main text and applying the factorization yields the Iceberg Limit equilibrium conditions:

$$\pi_{ni}^{j} = \frac{A_i^j w_i^{-\theta^j} (\tau_{ni}^j)^{-\theta^j}}{\sum_s A_s^j w_s^{-\theta^j} (\tau_{ns}^j)^{-\theta^j}}, \tag{A.20}$$

$$k_{ni}^{j} = \frac{\alpha^j X_n \pi_{ni}^j}{w_i \tau_{ni}^j}, \qquad k_{ni} = \sum_j k_{ni}^j, \qquad k_i = \sum_n k_{ni}, \tag{A.21}$$

$$P_n^j = \Gamma^j \Big(\sum_i A_i^j w_i^{-\theta^j} (\tau_{ni}^j)^{-\theta^j} \Big)^{-1/\theta^j}, \tag{A.22}$$

$$L_i = \sum_{n,j} k_{ni}^j \tau_{ni}^j + L_i^0, \qquad L_i^0 = \tfrac{\alpha^0}{\alpha} L_i, \tag{A.23}$$

$$\alpha X_n = w_n L_n, \qquad r_n H_n = \tfrac{1-\alpha}{\alpha} w_n L_n, \tag{A.24}$$

$$\frac{L_n}{\bar{L}} = \frac{H_n (w_n / P_n)^{\alpha/(1-\alpha)}}{\sum_{i=1}^{N-1} H_i (w_i / P_i)^{\alpha/(1-\alpha)}}. \tag{A.25}$$

Together with $P_n^0 = w_n / A_n^0$ and $k_{ni} = \sum_j k_{ni}^j$ and $k_i = \sum_n k_{ni}$, these define an *Iceberg Limit equilibrium* $\{w_n, r_n, L_n, X_n, P_n^j, \pi_{ni}^j, k_{ni}^j\}$ given the primitives $\{\alpha, \alpha^j, \sigma^j, A_n^j, \theta^j, \varphi_i^j, H_n, \bar{L}, L_N, c_{ni}, f_i\}$.

A.4 Computing Counterfactual Equilibria

Given primitives $\{\alpha, \alpha^j, \sigma^j, A_n^j, \theta^j, \varphi_i^j, H_n, \bar{L}, L_N, c_{ni}, \nu, f_i\}$ and starting values for nominal wages $\{w_i\}$ (with $w_1 = 1$) and transportation prices $\{t_{ni}\}$, the algorithm alternates an inner wage loop and an outer transportation-price loop. The steps below are computed over the set of bilateral pairs with positive trade in the baseline equilibrium.

1. Compute relative price indices P_1/P_n consistent with unit costs $\varphi_i^j w_i + t_{ni}$ and current wages, using the multi-sector aggregation (6) with the non-tradable price $P_n^0 = w_n / A_n^0$.

2. Compute trade shares π_{ni}^j from (5) at the current unit costs.

3. Compute U.S. population shares L_n/L_1 from (15) using the current $\{P_1/P_n\}$ and $\{w_n\}$; obtain L_n via the population constraint $\sum_n L_n = \bar{L}$, with L_N exogenous.

4. Compute total expenditure $X_n = w_n L_n / \alpha$ from trade balance (11).

5. Compute tons per market by sector $k_{ni}^j = \alpha^j X_n \pi_{ni}^j / (\varphi_i^j w_i + t_{ni})$ from (8); aggregate to $k_{ni} = \sum_j k_{ni}^j$ and $k_i = \sum_n k_{ni}$.

6. Update wages via $w_i^* = \sum_n \sum_j \alpha^j X_n \pi_{ni}^j / [L_i (1 - \alpha^0/\alpha)]$ (from (13)); iterate Steps 1–6 until $\|w^* - w\| < \epsilon$.

7. Update transportation prices by inverting the transport supply function: $t^*_{ni} = w_i\nu\log(k_{ni}/k_i) + w_i(c_{ni} + f_i)$; iterate Steps 1–7 until $\|t^* - t\| < \epsilon$.

For the Iceberg Limit ($\nu = 0$), the outer loop is unnecessary: Step 7 reduces to $t^*_{ni} = w_i(c_{ni} + f_i)$, independent of the transportation quantities.

Damped updates. Steps 6 and 7 are implemented as damped Picard updates, $x_{k+1} = (1-\lambda)\,x_k + \lambda\,T(x_k)$, with fixed relaxation. We use $\lambda_w = 0.05$ on the inner wage loop (Step 6) uniformly across initial-equilibrium and counterfactual computations; on the outer transportation-price loop (Step 7) we use $\lambda_t = 0.10$ for the initial equilibrium and $\lambda_t = 0.20$ for counterfactual experiments. Convergence is declared at $\|w^* - w\| < 10^{-11}$ on the inner loop and $\|t^* - t\| < 10^{-11}$ on the outer loop. Damping is necessary because the undamped iteration maps are not contractions at our calibration: direct finite-difference computation gives $\rho(M_{ww}) \approx 9.62$ at the Iceberg Limit and $\rho(DT_{\text{out}}) \approx 3.68$ at the baseline (Appendix A.5, "Numerical verification of regularity"). The damped scheme converges to the equilibrium whose local uniqueness is certified by the direct Jacobian non-singularity test in that section, even though the undamped iteration would not converge.

A.5 Proof of Proposition 1

Idea of the proof. At $\nu = 0$, transportation prices are pinned down by fundamentals, $t_{ni} = w_i(c_{ni} + f_i)$, and the full equilibrium system reduces to the Iceberg Limit system in (w, L) alone. Lemma 1 below delivers a solution (w^0, L^0) to that reduced system. The implicit function theorem then extends this solution to a C^∞ path $\nu \mapsto (w^*(\nu), L^*(\nu), t^*(\nu))$ on an open neighbourhood of $\nu = 0$, provided the equilibrium Jacobian is non-singular at the anchor. The Jacobian has a convenient block structure: at $\nu = 0$ its transport-price block is the identity, so non-singularity reduces via a Schur complement to non-singularity of the Iceberg Limit Jacobian J_0 (defined in Step 2 below)—a generic condition verified numerically at our calibrated parameters.

Existence of the Iceberg Limit equilibrium.

Lemma 1. *The Iceberg Limit system* (A.23)–(A.25) *admits an equilibrium with* $w^0 \gg 0$ *and* $L^0 \gg 0$.

Proof. Equilibrium residuals. Rewrite the full-employment (13) and population-mobility (15) conditions as residuals of the endogenous (w, L, t):

$$G^w_i(w, L, t) \equiv (1 - \tfrac{\alpha^0}{\alpha})\, w_i L_i - \sum_{n=1}^{N}\sum_{j=1}^{J} \alpha^j\, \pi^j_{ni}(w, t)\, X_n(w, L), \quad i = 2, \ldots, N,$$

$$G^L_n(w, L, t) \equiv \frac{L_n}{\bar{L}} - \frac{H_n(w_n/P_n(w,t))^{\alpha/(1-\alpha)}}{\sum_{m=1}^{N-1} H_m(w_m/P_m(w,t))^{\alpha/(1-\alpha)}}, \quad n = 1, \ldots, N-1,$$

with $w_1 = 1$, L_N exogenous, $X_n = w_n L_n/\alpha$, and π^j_{ni}, P_n the functions of (w,t) defined by (5) and (6). Setting $t = t^0$ with $t^0_{ni} \equiv w_i(c_{ni} + f_i)$ collapses the unit cost $\varphi^j_i w_i + t_{ni}$ to $w_i \tau^j_{ni}$, where $\tau^j_{ni} \equiv \varphi^j_i + c_{ni} + f_i$, so $G^w(\cdot,\cdot,t^0) = 0$ and $G^L(\cdot,\cdot,t^0) = 0$ are exactly the Iceberg Limit system (A.23)–(A.25). The lemma is the claim that this reduced system has a solution (w^0, L^0) with $w^0 \gg 0$ and $L^0 \gg 0$.

Reduction to wages alone. $G^L(w, L, t^0) = 0$ determines populations as a continuous function of wages,

$$L_n = \Lambda_n(w) \equiv \bar{L}\,\frac{H_n(w_n/P_n(w))^{\alpha/(1-\alpha)}}{\sum_{m=1}^{N-1} H_m(w_m/P_m(w))^{\alpha/(1-\alpha)}} \quad (n < N), \qquad \Lambda_N \equiv L_N,$$

with $P_n(w)$ the Iceberg Limit price index (A.22) evaluated at τ^j_{ni}. By construction $\Lambda_n(w) > 0$ on $\mathbb{R}^N_{++}$ and $\sum_{n=1}^{N-1} \Lambda_n(w) = \bar{L}$. Substituting $L = \Lambda(w)$ into $G^w(w, L, t^0) = 0$ and dividing through by w_i yields the labor excess-demand system

$$Z_i(w) \equiv \frac{1}{w_i} \sum_{n=1}^{N} \sum_{j=1}^{J} \alpha^j\, \pi^j_{ni}(w)\, X_n(w) \;-\; \big(1 - \tfrac{\alpha^0}{\alpha}\big)\, \Lambda_i(w) = 0, \qquad i = 1, \ldots, N,$$

with $\pi^j_{ni}(w)$ the Iceberg Limit trade share (A.20) and $X_n(w) = w_n \Lambda_n(w)/\alpha$. We verify four properties of Z.

(i) *Continuity.* $Z : \mathbb{R}^N_{++} \to \mathbb{R}^N$ is C^∞: trade shares and price indices are rational functions of positive powers of wages, and $\Lambda_n(w)$ inherits smoothness from $P_n(w)$.

(ii) *Homogeneity of degree zero.* Trade shares $\pi^j_{ni}(w)$ are homogeneous of degree zero because the $w_s^{-\theta^j}$ factors cancel between numerator and denominator of (A.20); $P_n(w)$ is homogeneous of degree one, so $w_n/P_n(w)$ and hence $\Lambda_n(w)$ are homogeneous of degree zero. Each term in Z_i is therefore degree-zero, so $Z(\lambda w) = Z(w)$ for all $\lambda > 0$; we may normalise $w_1 = 1$.

(iii) *Walras's law.* Using $\sum_i \pi^j_{ni} = 1$, $\sum_{j=1}^{J} \alpha^j = \alpha - \alpha^0$, and $X_n = w_n \Lambda_n(w)/\alpha$,

$$\sum_{i=1}^{N} w_i Z_i(w) = \sum_{n=1}^{N} (\alpha - \alpha^0) X_n(w) - \big(1 - \tfrac{\alpha^0}{\alpha}\big) \sum_{i=1}^{N} w_i \Lambda_i(w) = \big(1 - \tfrac{\alpha^0}{\alpha}\big)\Big[\sum_n w_n \Lambda_n - \sum_i w_i \Lambda_i\Big] = 0,$$

since the two bracketed sums coincide under the same index.

(iv) *Boundary repulsion.* Fix $w_k > 0$ for $k \neq i$ and let $w_i \to 0$. The term $A^j_i w_i^{-\theta^j} (\tau^j_{ni})^{-\theta^j}$ in the denominator of (A.20) diverges while the remaining terms of that denominator are bounded, so $\pi^j_{ni}(w) \to 1$ for every destination n and sector j, and total tradable revenue at origin i approaches $\sum_{n=1}^{N} (\alpha - \alpha^0) X_n(w)$. This limit is bounded below by a strictly positive constant: wages and populations at $n \neq i$ stay away from zero

(other wages are fixed and $\Lambda_n(w) \to \bar{L} \cdot H_n(w_n/P_n)^{\alpha/(1-\alpha)} / \sum_{m \neq i} H_m(w_m/P_m)^{\alpha/(1-\alpha)} > 0$ since location i's real wage $w_i/P_i \to 0$ so its share of the population denominator vanishes). Dividing this bounded-below revenue by $w_i \to 0$ sends the first term of $Z_i(w)$ to $+\infty$, while the second term $(1 - \alpha^0/\alpha)\Lambda_i(w) \to 0$ because $w_i/P_i \to 0$ drives $\Lambda_i(w)$ to zero. Hence $Z_i(w) \to +\infty$, and the boundary $\{w_i = 0\}$ is repelling.

Conclusion. By Proposition 17.C.1 of Mas-Colell et al. (1995), (i)–(iv) imply the existence of $w^0 \gg 0$ with $Z(w^0) = 0$.[3] Setting $L^0 \equiv \Lambda(w^0)$ gives $L^0 \gg 0$ and $G^L(w^0, L^0, t^0) = 0$ by construction; multiplying $Z(w^0) = 0$ through by w_i^0 recovers $G^w(w^0, L^0, t^0) = 0$. Hence (w^0, L^0) solves the Iceberg Limit system (A.23)–(A.25). □

Regularity condition. Let J_0 denote the Jacobian of the reduced Iceberg Limit system (A.23)–(A.25) at (w^0, L^0). We say the Iceberg Limit equilibrium is *regular* when $\det(J_0) \neq 0$. Regularity is strictly weaker than uniqueness: if the Iceberg Limit has multiple equilibria, each regular, Proposition 1 applies separately to each.

Proof of Proposition 1.

Proof. Take G^w, G^L from the proof of Lemma 1 and add the transport-supply residual

$$G^t_{ni}(w, L, t; \nu) \equiv t_{ni} - w_i \, \nu \, \log\big(k_{ni}(w, L, t)/k_i(w, L, t)\big) - w_i(c_{ni} + f_i), \quad n, i = 1, \ldots, N,$$

with k_{ni}, k_i the functions of (w, L, t) defined by (8). A competitive equilibrium with transportation markets corresponds to (w, L, t) on the admissible domain with $G(w, L, t; \nu) \equiv (G^w, G^L, G^t) = 0$; G^w, G^L, and G^t have $N-1$, $N-1$, and N^2 components, matching the $2(N-1) + N^2$ unknowns. Set $t^0_{ni} \equiv w^0_i(c_{ni} + f_i)$ and partition the Jacobian:

$$\frac{\partial G}{\partial(w, L, t)} = \begin{pmatrix} A & B \\ C & D \end{pmatrix}, \qquad D \equiv \left.\frac{\partial G^t}{\partial t}\right|_{\nu=0}.$$

Step 1 (anchor and block D). Lemma 1 delivers $G^w(w^0, L^0, t^0) = 0$ and $G^L(w^0, L^0, t^0) = 0$; G^t vanishes at $(w^0, L^0, t^0; 0)$ because its logarithmic term is multiplied by ν and therefore vanishes at $\nu = 0$, and $t^0_{ni} = w^0_i(c_{ni} + f_i)$ by construction. Differentiating G^t_{ni} in t produces the identity plus a term multiplied by ν, which vanishes at $\nu = 0$; hence $D = I_{N^2}$.

Step 2 (Schur identification with J_0). Since $D = I$ is non-singular, $\det(\partial G/\partial(w, L, t)) = \det(D) \cdot \det(A - BD^{-1}C) = \det(A - BC)$. At $\nu = 0$ the transport block defines t as an explicit function of w alone, $t_{ni} = w_i(c_{ni} + f_i)$. By the chain rule,

[3] MWG Prop. 17.C.1 invokes Kakutani's fixed-point theorem on a price-simplex correspondence, yielding exact market clearing $Z(w^0) = 0$; the Brouwer-based Prop. 17.C.2 would give only the weaker free-disposal conclusion. This is the same MWG result used by Alvarez and Lucas (2007) for the Eaton–Kortum model with tariffs and intermediates.

the Jacobian of the reduced Iceberg Limit system in (w, L) is $J_0 = A + B\,\partial t/\partial(w, L)|_{\nu=0}$. Differentiating $G^t = t - w(c + f)$ directly in (w, L) gives $C = -\partial t/\partial(w, L)|_{\nu=0}$, so the Schur complement equals J_0. By the regularity condition, $\det(J_0) \neq 0$, hence $\det(\partial G/\partial(w, L, t)) \neq 0$ at $\nu = 0$.

Step 3 (implicit function theorem). G is C^∞ on the admissible domain $\{w \gg 0,\ L \gg 0,\ \varphi_i^j w_i + t_{ni} > 0,\ k_{ni} > 0,\ k_i > 0\}$. By the IFT, there exists $\bar{\nu} > 0$ and a unique C^∞ function $\nu \mapsto (w^*(\nu), L^*(\nu), t^*(\nu))$ on a neighbourhood of $\nu = 0$ with $G = 0$; the path is locally unique and reduces to the Iceberg Limit anchor at $\nu = 0$.

Step 4 (admissibility). At $\nu = 0$, all admissibility constraints hold strictly; continuity of (w^*, L^*, t^*) in ν preserves them on a neighbourhood of zero. Restricting $\bar{\nu}$ if necessary, the path delivers a locally unique competitive equilibrium with transportation markets for every $\nu \in [0, \bar{\nu})$. □

Comparison with the global spectral-radius approach. Allen et al. (2024) (AAL) develop a sufficient condition for global existence and uniqueness in canonical spatial systems of the form $x_{ih} = \sum_j f_{ijh}(x_{j1}, \ldots, x_{jH})$, where each kernel f_{ijh} depends only on the row x_j at the source location. The condition is $\rho(\mathbf{A}^\star) < 1$, with $\mathbf{A}^\star$ a non-negative $H \times H$ matrix whose entries upper-bound the kernel elasticities $|\partial \ln f_{ijh}/\partial \ln x_{jh'}|$ uniformly. This condition fails in our setting.

Reduction to $H = 2$. At $\nu = 0$, $t_{ni} = w_i(c_{ni} + f_i)$ eliminates the transport-price block, and under a common trade elasticity $\theta^j = \theta$ the Iceberg Limit system collapses to two equations per location. Setting $x_{i1} \equiv w_i^{1+\theta} L_i$ and $x_{i2} \equiv L_i$ (a smooth bijection on $\mathbb{R}^2_{++}$), full employment and population mobility take the AAL canonical form

$$x_{i1} = \sum_n K_{in}^{(1)}\, x_{n1}^{1/(1+\theta)} x_{n2}^{\theta/(1+\theta)}, \qquad x_{n2} = \tilde{K}_n^{(2)}\, x_{n1}^{c}, \qquad c \equiv \frac{\alpha}{1 + \theta(1-\alpha)},$$

where $K_{in}^{(1)}$ absorbs $(\alpha^j, A_i^j, \tau_{ni}^j, \Phi_n^j)$ and $\tilde{K}_n^{(2)}$ absorbs (H_n, P_n, D). Sectoral heterogeneity drops out of the canonical form via the common-θ assumption.

Chain-rule corrections and spectral radius. The kernels themselves depend on x_n through Φ_n^j, P_n, and D, so the AAL bound must dominate the full elasticities including these feedbacks. Computing them (using $\partial \ln \Phi_n^j/\partial \ln w_n = -\theta\, \pi_{nn}^j$ and analogous identities) and taking elementwise suprema over $(\pi_{nn}^j, \pi_{nn}, \sigma_n) \in [0, 1]^3$ with $\sigma_n \equiv L_n/\bar{L}$, the valid AAL upper-bound matrix is

$$\mathbf{A}^\star = \begin{pmatrix} 1 & \theta/(1+\theta) \\ c & c \end{pmatrix}, \qquad \rho(\mathbf{A}^\star) = \tfrac{1}{2}\big[(1+c) + \sqrt{(1+c)^2 - 4c/(1+\theta)}\big].$$

The inequality $\rho(\mathbf{A}^\star) > 1$ is equivalent to $4c\theta/(1+\theta) > 0$, true for any $\theta, \alpha > 0$. At our calibration ($\theta \approx 5$, $\alpha = 0.75$, $c = 1/3$), $\rho(\mathbf{A}^\star) \approx 1.29$, about 29% above the AAL

threshold.

Heterogeneous θ^j and extension to $\nu > 0$. If θ^j varies across sectors, taking $\theta = \sup_j \theta^j$ only loosens the bound, so $\rho(\mathbf{A}^\star) > 1$ continues to hold. For $\nu > 0$, the implicit function theorem applied to $G^t = 0$ at $\nu = 0$ (where $\partial G^t/\partial t = I_{N^2}$, by Step 1 of the proof above) gives a smooth extension $t_{ni}(w, L; \nu)$; the entries of $\mathbf{A}^\star(\nu)$ depend continuously on ν, so $\rho(\mathbf{A}^\star(\nu)) > 1$ persists for ν small. AAL's sufficient condition therefore cannot certify existence and uniqueness in our model at the Iceberg Limit or at any ν sufficiently close to it.

This does *not* imply multiplicity of equilibria: AAL's multiplicity result (their Thm. 1, part (iii)) is existential—it constructs a second solution for a *specific* choice of kernel constants $\{K_{ijh}\}$ and does not transfer to systems whose kernels are correlated through shared primitives.[4] Other global approaches also fail to apply. Allen and Arkolakis (2014) Theorem 1 proves existence and uniqueness via a Perron–Frobenius / Krein–Rutman argument on a pair of linear integral operators whose kernels are transposes of one another; this transpose-link is a feature of the single-sector CES gravity equilibrium and breaks under our multi-sector extension, which yields J coupled operators without a pairwise transpose relation. Their Theorem 2 collapses the nonlinear system to a single Hammerstein integral equation via an algebraic identity that requires symmetric trade costs $T(i, j) = T(j, i)$; our fundamental costs are directionally asymmetric ($c_{ni} \neq c_{in}$ in general), so the identity does not hold. The gross-substitutes approach of Alvarez and Lucas (2007) (their Theorem 3, via Prop. 17.F.3 of Mas-Colell et al. 1995) requires reducing the system to a wage-only excess demand, which in our model would demand closed-form elimination of t_{ni}; the inverse-supply relation $t_{ni} = w_i \nu \log(k_{ni}/k_i) + w_i(c_{ni} + f_i)$ defines t_{ni} only implicitly at $\nu > 0$ through the dependence of k_{ni}, k_i on (w, L, t). Each global tool requires model-specific structure that our setting lacks. We therefore adopt the local IFT approach, which requires only that J_0 be non-singular at the calibrated anchor.

Numerical verification of regularity. We verify the conditions of Proposition 1 at the calibrated parameters by direct finite-difference computation of the equilibrium Jacobian. The Jacobian is evaluated at two anchor points: the Iceberg Limit equilibrium (w^0, L^0) at $\nu = 0$, which certifies the regularity hypothesis of Proposition 1, and the baseline equilibrium $(\hat{w}, \hat{L}, \hat{t})$ at $\hat{\nu} = 0.103$, which certifies local uniqueness of the calibrated equilibrium directly. Both equilibria are computed by the algorithm of Appendix A.4.

At $\nu = 0$, we compute the Jacobian $\tilde{J}_0$ of the reduced Iceberg Limit system in wages alone (after substituting out L, whose block is trivially invertible since population mobility has the form $L - \Lambda(w)$). Central finite differences on the Dekle–Eaton–

[4] AAL Online Appendix A.3 (footnote 10) makes exactly this caveat: $\rho(\mathbf{A}^\star) > 1$ does not imply multiplicity when the $\{K_{ijh}\}$ are correlated through shared primitives, as ours are. Their explicit multiplicity construction (their Appendix A.2) additionally requires positive agglomeration spillovers, absent from our Helpman-housing formulation.

Kortum hat-algebra representation, with step size 10^{-6} (stable across $[10^{-8}, 10^{-4}]$), give $\min_{\lambda \in \mathrm{spec}(\tilde{J}_0)} |\lambda| \approx 3.76$ and $\log_{10} |\det(\tilde{J}_0)| \approx 104.2$. The regularity condition holds with wide slack.

At $\hat{\nu} = 0.103$, the full equilibrium Jacobian factors via Schur complement into $\det(I - M_{ww}) \cdot \det(I - DT_{\text{out}})$, with M_{ww} the wage-iteration Jacobian at fixed t and $DT_{\text{out}} = N_{tt} + N_{tw}(I - M_{ww})^{-1} M_{wt}$ assembled from finite differences on the combined one-step map. Direct evaluation gives $\min |\mathrm{spec}(I - M_{ww})| \approx 3.12$; Arnoldi iteration applied to a matrix-free linear operator that implements DT_{out} via the identity above finds $\rho(DT_{\text{out}}) \approx 3.68$, with the top eigenvalues in $|\lambda| \in [1.44, 3.68]$ and bounded away from 1. Matrix-free GMRES on $(I - DT_{\text{out}})x = b$ for a random b returns relative residual $\approx 9 \times 10^{-10}$, directly certifying $\det(I - DT_{\text{out}}) \neq 0$. The full Jacobian at $\hat{\nu}$ is therefore non-singular and the calibrated baseline is locally unique. These spectral magnitudes also explain why the iteration of Appendix A.4 requires damping: the undamped Picard map is not a contraction at our calibration.

A.6 Proof of Proposition 2

Proof. Substituting $t_{ni}/w_i = c_{ni} + f_i$ from (A.18) gives $\varphi_i^j w_i + t_{ni} = w_i \tau_{ni}^j$, with $\tau_{ni}^j \equiv \varphi_i^j + c_{ni} + f_i$.

Part (i). Set $\alpha^0 = 0$ (only tradables, $\sum_{j \geq 1} \alpha^j = \alpha = 1$, $L_i^0 = 0$) and let L_n be exogenous. The price-indexed demand (A.21) gives $w_i \tau_{ni}^j k_{ni}^j = \pi_{ni}^j \alpha^j X_n$. Full employment (A.23) then becomes

$$w_i L_i = \sum_n \sum_j \pi_{ni}^j \alpha^j w_n L_n, \tag{A.26}$$

under trade balance $\alpha X_n = w_n L_n$, with trade shares $\pi_{ni}^j = A_i^j w_i^{-\theta^j} (\tau_{ni}^j)^{-\theta^j} \big/ \sum_s A_s^j w_s^{-\theta^j} (\tau_{ns}^j)^{-\theta^j}$. Equations (A.26) and the preceding trade-share formula coincide with equations (4) and (6) of Costinot et al. (2012).

Part (ii). Set $J = 1$, $\alpha^0 = 0$ (so $\alpha = 1$), and drop sector superscripts with $\tau_{ni} = \varphi_i + c_{ni} + f_i$. The equilibrium conditions of our Iceberg Limit then map term-by-term to those of Allen and Arkolakis (2014) in the no-spillovers case ($\beta = 0$ in their notation), with H_n acting as the land endowment in the congestion channel: trade shares (A.20) $\leftrightarrow$ AA14 (5), full employment (A.26) $\leftrightarrow$ AA14 (6), population mobility (A.25) $\leftrightarrow$ AA14 (7). □

A.7 Proof of Proposition 3

Proof. Common utility across locations is $\bar{u} = \left[\sum_n H_n (w_n/P_n)^{\alpha/(1-\alpha)}\right]^{1-\alpha}$, and totally differentiating, using the population-mobility condition $L_n/\bar{L} = H_n (w_n/P_n)^{\alpha/(1-\alpha)}/D$

with $D \equiv \sum_m H_m (w_m/P_m)^{\alpha/(1-\alpha)}$,

$$d\ln \bar{u} = \alpha \sum_n \tfrac{L_n}{\bar{L}}\, d\ln(w_n/P_n). \tag{A.27}$$

Using (5) and (6), the domestic trade share satisfies $\pi^j_{nn} = A^j_n (\Gamma^j)^{-\theta^j} (w_n/P^j_n)^{-\theta^j} (\tau^j_{nn})^{-\theta^j}$, so $w_n/P^j_n = (A^j_n)^{1/\theta^j} \big/ \big[\Gamma^j\, \tau^j_{nn}\, (\pi^j_{nn})^{1/\theta^j}\big]$. Aggregating with $w_n/P_n = \prod_{j=0}^{J} (w_n/P^j_n)^{\alpha^j/\alpha}$ and using $w_n/P^0_n = A^0_n$, we obtain

$$d\ln(w_n/P_n) = -\sum_{j=1}^{J} \tfrac{\alpha^j}{\alpha}\Big[\tfrac{1}{\theta^j} d\ln \pi^j_{nn} + d\ln \tau^j_{nn}\Big]. \tag{A.28}$$

Substituting (A.28) into (A.27) yields (17) of the main text. □

A.8 Symmetric Setting and Proof of Proposition 4

Symmetric setting. We use the symmetric specification of the baseline model for the analytical comparative statics of Proposition 4 and the numerical example in Section 3.3. All locations and sectors are identical; we normalise $w = 1$, $A = A^0 = H = 1$; each origin has only two transportation markets, one *internal* ($i = n$) and $N - 1$ identical *external* ($i \neq n$) markets, differing only in fundamental costs (c_{nn} vs. c_{ni}). Writing $r \equiv (\varphi + t_{\mathrm{nn}})/(\varphi + t_{\mathrm{ni}})$ and $s_{\mathrm{nn}} \equiv k_{\mathrm{nn}}/k$, $s_{\mathrm{ni}} \equiv k_{\mathrm{ni}}/k$ for the truck shares,

$$\frac{\pi_{\mathrm{nn}}}{\pi_{\mathrm{ni}}} = r^{-\theta}, \qquad \text{(trade-share ratio, from (5))} \tag{A.29}$$

$$\frac{k_{\mathrm{ni}}}{k_{\mathrm{nn}}} = r^{\theta+1}, \qquad \text{(transport-demand ratio, from (8))} \tag{A.30}$$

$$s_{\mathrm{nn}} + (N-1) s_{\mathrm{ni}} = 1, \qquad \text{(free entry (10))} \tag{A.31}$$

$$L\big(1 - \tfrac{\alpha^0}{\alpha}\big) = \varphi\, k + t_{\mathrm{nn}} k_{\mathrm{nn}} + (N-1)\, t_{\mathrm{ni}} k_{\mathrm{ni}}, \qquad \text{(full employment)} \tag{A.32}$$

$$L/\bar{L} = 1/N, \qquad \text{(population mobility)} \tag{A.33}$$

$$\frac{s_{\mathrm{ni}}}{s_{\mathrm{nn}}} = \exp\Big[\tfrac{t_{\mathrm{ni}} - c_{\mathrm{ni}} - t_{\mathrm{nn}} + c_{\mathrm{nn}}}{\nu}\Big], \qquad \text{(supply ratio, from (9))} \tag{A.34}$$

An equilibrium is $(t_{\mathrm{nn}}, t_{\mathrm{ni}}, k, k_{\mathrm{nn}}, k_{\mathrm{ni}}, \pi_{\mathrm{nn}}, \pi_{\mathrm{ni}}, L, r, P, P^0)$ satisfying these conditions together with the symmetric price indices $P = \Gamma[A(\varphi + t_{\mathrm{nn}})^{-\theta} + (N-1)A(\varphi + t_{\mathrm{ni}})^{-\theta}]^{-1/\theta}$ and $P^0 = 1/A^0$, and the demand relations $k_{\mathrm{nn}} = ((\alpha - \alpha^0)/\alpha)\, L\, \pi_{\mathrm{nn}}\, (\varphi + t_{\mathrm{nn}})^{-1}$ and $k_{\mathrm{ni}} = ((\alpha - \alpha^0)/\alpha)\, L\, \pi_{\mathrm{ni}}\, (\varphi + t_{\mathrm{ni}})^{-1}$.

Proof of Proposition 4.

Proof. Differentiating with respect to c_{ni}, holding c_{nn} and f fixed. Let $\rho \equiv dt_{\mathrm{ni}}/dt_{\mathrm{nn}}$.

(i) $dt_{\mathbf{ni}} < dt_{\mathbf{nn}} < 0$**.** Totally differentiating the demand ratio (A.30) and the supply ratio $s_{\rm ni}/s_{\rm nn} = \exp[(t_{\rm ni} - c_{\rm ni} - t_{\rm nn} + c_{\rm nn})/\nu]$, and equating, yields

$$(\theta+1)\frac{\pi_{\rm ni}}{\pi_{\rm nn}}\,\frac{dt_{\rm nn}(\varphi+t_{\rm ni}) - dt_{\rm ni}(\varphi+t_{\rm nn})}{(\varphi+t_{\rm ni})^2} = \frac{s_{\rm ni}}{s_{\rm nn}}\left(\frac{dt_{\rm ni} - dc_{\rm ni} - dt_{\rm nn}}{\nu}\right). \tag{A.35}$$

Differentiating the free entry condition (10) under symmetry ($df = 0$, $dc_{\rm nn} = 0$) gives

$$dt_{\rm ni} - dc_{\rm ni} = \frac{-s_{\rm nn}\,dt_{\rm nn}}{(N-1)s_{\rm ni}}, \tag{A.36}$$

and we observe that $dt_{\rm nn} \neq 0$ (otherwise (A.36) forces $dt_{\rm ni} = dc_{\rm ni} < 0$, contradicting (A.35), whose LHS is strictly positive and RHS zero). Substituting (A.36) into the RHS of (A.35) and using $s_{\rm nn} + (N-1)s_{\rm ni} = 1$ gives

$$\rho = \frac{(\theta+1)\,\pi_{\rm ni}/\pi_{\rm nn}\,(\varphi+t_{\rm ni})^{-1} + [(N-1)\nu s_{\rm nn}]^{-1}}{(\theta+1)\,\pi_{\rm ni}/\pi_{\rm nn}\,(\varphi+t_{\rm nn})/(\varphi+t_{\rm ni})^2}. \tag{A.37}$$

$\rho > 1$ follows by comparing the first numerator term to the denominator and using $t_{\rm ni} > t_{\rm nn}$ (which holds whenever $c_{\rm ni} > c_{\rm nn}$, since the function $g(t) \equiv \nu(\theta+1)\ln(\varphi+t) + t$ is strictly increasing and $g(t_{\rm nn}) = g(t_{\rm ni}) - (c_{\rm ni} - c_{\rm nn})$). Sign of $dt_{\rm nn}$: if $dt_{\rm nn} \geq 0$, then $dt_{\rm ni} \geq 0$ (by $\rho > 0$) and (A.36) is contradicted (LHS> 0, RHS≤ 0). Therefore $dt_{\rm nn} < 0$ and $dt_{\rm ni} < dt_{\rm nn} < 0$.

(ii) $d\pi_{\mathbf{nn}} < 0 < d\pi_{\mathbf{ni}}$**.** Writing $\pi_{\rm nn}/\pi_{\rm ni} = r^{-\theta}$ with $r \equiv (\varphi+t_{\rm nn})/(\varphi+t_{\rm ni})$, it suffices to show r increases, i.e. $dt_{\rm ni}/(\varphi+t_{\rm ni}) < dt_{\rm nn}/(\varphi+t_{\rm nn})$. Dropping the positive second term in the numerator of (A.37) gives $\rho > (\varphi+t_{\rm ni})/(\varphi+t_{\rm nn})$, which (with $dt_{\rm nn} < 0$) delivers the inequality. Combined with $\pi_{\rm nn} + (N-1)\pi_{\rm ni} = 1$, this implies $d\pi_{\rm nn} < 0 < d\pi_{\rm ni}$.

(iii) $dk > 0$ **for** N **sufficiently large.** From (A.32), $k = \tilde{L}/D$ with $\tilde{L} \equiv L(1-\alpha^0/\alpha)$ and $D \equiv \varphi + t_{\rm nn}s_{\rm nn} + (N-1)t_{\rm ni}s_{\rm ni}$. Since $\tilde{L}$ is fixed, $dk > 0$ iff $dD < 0$. Using $s_{\rm nn} = 1 - (N-1)s_{\rm ni}$ to write $D = \varphi + t_{\rm nn} + (N-1)(t_{\rm ni} - t_{\rm nn})s_{\rm ni}$ and differentiating,

$$dD = \underbrace{dt_{\rm nn} + (N-1)(dt_{\rm ni} - dt_{\rm nn})s_{\rm ni}}_{\text{direct } (<0)} + \underbrace{(N-1)(t_{\rm ni} - t_{\rm nn})\,ds_{\rm ni}}_{\text{composition } (>0)}. \tag{A.38}$$

From (A.36) with $df = 0$, $ds_{\rm ni} = -s_{\rm nn}\,dt_{\rm nn}/[(N-1)\nu]$. A sequence of substitutions—expressing ρ via (A.37), using the identity $\varphi + t_{\rm ni} = D + s_{\rm nn}(t_{\rm ni} - t_{\rm nn})$, and collecting terms—reduces (A.38) to[5]

$$dD = \frac{D\,dt_{\rm nn}}{\nu}\left[\frac{\nu}{\varphi+t_{\rm nn}} + 1 - \frac{\theta(\varphi+t_{\rm ni})}{(\theta+1)D}\right]. \tag{A.39}$$

[5]Detailed arithmetic: define Term A $\equiv (N-1)s_{\rm ni}(r^{-1}-1)$ and Term B $\equiv s_{\rm ni}(\varphi+t_{\rm ni})r^{-\theta-1}/[\nu s_{\rm nn}(\theta+1)]$; then $(N-1)s_{\rm ni}(\rho-1) = $ A+B. Using $r^{-1}-1 = (t_{\rm ni}-t_{\rm nn})/(\varphi+t_{\rm nn})$, one obtains $1+$A$ = D/(\varphi+t_{\rm nn})$, and $s_{\rm ni}/s_{\rm nn} = r^{\theta+1}$ (from the supply-demand equilibrium) gives B $= (\varphi+t_{\rm ni})/[(\theta+1)\nu]$. Substituting and applying the identity $\varphi + t_{\rm ni} = D + s_{\rm nn}(t_{\rm ni} - t_{\rm nn})$ yields (A.39).

Since $dt_{\text{nn}} < 0$ and $D > 0$, $dD < 0$ whenever the bracket is positive. The first bracket term is strictly positive, so a sufficient condition is $D > \theta(\varphi + t_{\text{ni}})/(\theta + 1)$. Expressed in terms of r,

$$(N-1)r^{\theta+1} + (\theta+1)r > \theta. \tag{A.40}$$

Equating (A.30) with the supply ratio and taking logs yields $\nu(\theta+1)\ln(1/r)+(\varphi+t_{\text{ni}})(1-r) = c_{\text{ni}} - c_{\text{nn}}$; both LHS terms are non-negative, so $r \geq \underline{r}(\nu) \equiv \exp[-(c_{\text{ni}} - c_{\text{nn}})/(\nu(\theta+1))] > 0$, a bound independent of N. Therefore $(N-1)r^{\theta+1} \to \infty$ as $N \to \infty$ and (A.40) holds for N large. For the parameter values in Table 1, (A.40) is satisfied with a wide margin. □

A.9 Parameterization of the Numerical Example

All locations and sectors are identical, so each $L_n = \bar{L}/N$, $H_n = 1$, and the only market types are internal and external (see "Symmetric setting" in Subsection A.8). We obtain parameter values for the symmetric setting (Section 3.3) by averaging the corresponding location- or sector-specific primitives from the full calibration (Section 4.4): $\nu = 0.103$ (estimated in Section 4.2); $\theta = (1/J)\sum_j \theta^j$; c_{nn} and c_{ni} as the means of $\tilde{c}_{nn}$ and $\tilde{c}_{ni}$ respectively, with $\tilde{c}_{ni}$ from (20); φ and f as means across locations; normalisations $A = A^0 = H = w = 1$. The resulting values appear in Table 1.

Parameter	Description	Value
N	Number of locations	129
ν	Cost heterogeneity (inverse supply elasticity)	0.103
θ	Trade elasticity, avg. across $J = 16$ sectors	8.606
φ	Labor per truck, avg. across locations	2.374
f	Entry cost per truck, avg. across locations	0.547
c_{nn}	Internal fundamental cost, avg.	0.054
c_{ni}	External fundamental cost, avg.	1.103
α	Total expenditure share on goods	0.750
α^0	Expenditure share on non-tradables	0.597
A, H, w	Normalised	1

Table 1: Parameter Values for the Symmetric Numerical Example (Section 3.3).

B Data, Estimation, and Identification

This appendix documents data sources, the identification arguments behind the instrument and the level of fundamental costs, and the inversions used to calibrate the non-estimated parameters; it also reports robustness exercises for the empirical analysis. We calibrate the model to 128 U.S. regions and 1 Canadian region (129 locations) with 17 sectors (16 tradable + 1 service) classified according to the North American Industry

Classification System (NAICS), matching the tradable sectors of Caliendo et al. (2018) except for Agriculture, which we take from Caliendo and Parro (2015).

B.1 Transportation Prices

We web-scrape shipping quotes from Schneider's FreightPower platform on 2022 queries for a standardised shipment (see main text, Section 4.1, for the full list of held-constant shipment parameters). The U.S. Freight Analysis Framework (FAF5), produced by the Bureau of Transportation Statistics (BTS) and Federal Highway Administration (FHWA), provides our 128 U.S. regions. FAF5 regions are mapped to ZIP codes using the U.S. Department of Housing and Urban Development (HUD) and U.S. Postal Service (USPS) crosswalk, choosing the ZIP with the most residential addresses; for Canadian origins/destinations we select ZIPs in the five largest urban centres (Toronto, Montreal, Vancouver, Calgary, Ottawa) and average internal Canadian quotes across them. We deflate 2022 quotes to 2017 dollars using the Bureau of Labor Statistics (BLS) producer price index for general freight trucking.

B.2 Validation against USDA Truck Rate Data

We benchmark our Schneider quotes against the U.S. Department of Agriculture (USDA) Agricultural Marketing Service (AMS) *Fruit and Vegetable Truck Rate Report* (FVWTRK, Socrata dataset `acar-e3r8`), a weekly government-collected series of spot-market truckload rates for refrigerated produce between ~ 20 U.S. production districts and 10 terminal-market destinations. Mapping USDA origins/destinations to FAF5 zones and averaging rates across commodities, weeks, and origins sharing the same FAF5 zone, we obtain 148 matched lanes for May 2017 and 122 for May 2022.

The two sources differ in *which shipment parameters are held constant*: Schneider fixes commodity, weight, dimensions, equipment type, and service level; USDA holds none of these constant (a single USDA entry can bundle up to 22 produce items, pools 48-ft and 53-ft refrigerated trailers, and varies load weight and carrier type within the week). Because transportation services on a given market are close substitutes in production, market-specific fundamental costs should drive cross-market covariance between the two sources even though price levels and bundle compositions differ. Figure 1 plots standardised prices (z-scores on the matched-lane subsample) of the two series. The Pearson correlation is 0.45 in 2017 (Panel (a)) and 0.63 in 2022 (Panel (b)); Spearman rank correlations are 0.56 and 0.65 respectively. With standardised series the OLS slope equals the Pearson correlation exactly. These positive correlations validate the Schneider cross-market price variation that identifies ν and $\tilde{c}_{ni}$ in our 2SLS specification (equation (19)), which includes origin fixed effects.

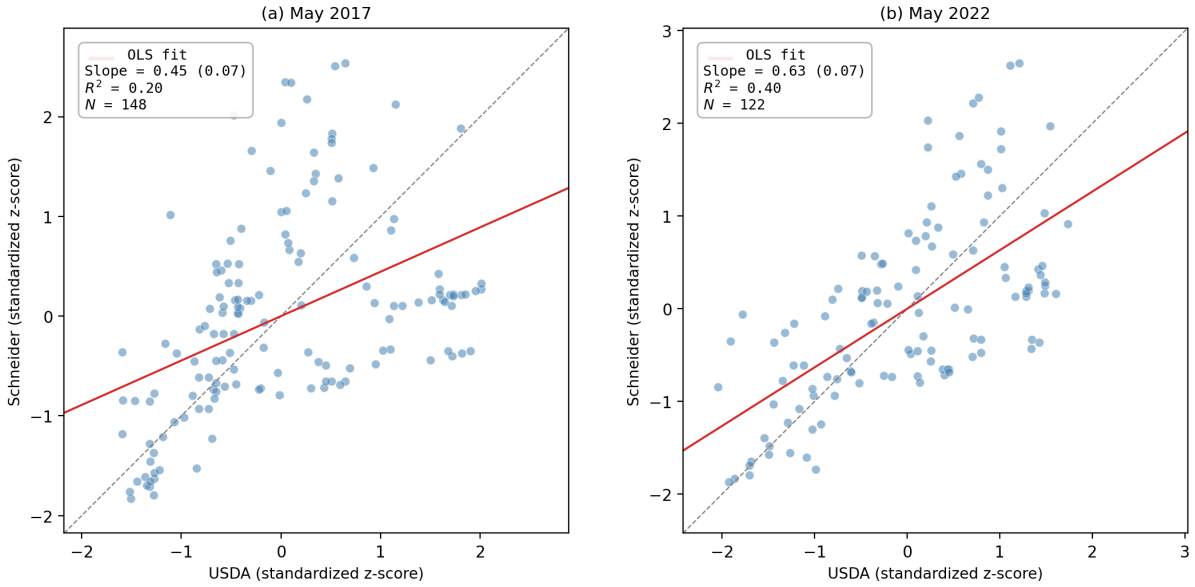

Figure 1: Standardised prices on matched origin-destination lanes. Panel (a): May 2017 (148 lanes). Panel (b): May 2022 (122 lanes). Each series is demeaned and divided by its own sample SD on the matched-lane subsample, so the OLS slope equals the Pearson correlation.

Invariance to measurement error in observed t_{ni}. The estimated transportation supply elasticity and the counterfactual welfare percentage changes are invariant to additive measurement error of the form $t_{ni}^{\text{obs}} = t_{ni}^{\text{true}} + a_i$ (with a_i an origin-specific constant) and to multiplicative measurement error $t_{ni}^{\text{obs}} = s \cdot t_{ni}^{\text{true}}$ ($s > 0$).

Identification. The additive case adds the constant a_i/w_i to the dependent variable in the inverse-supply regression (19); the origin fixed effects absorb it, so $\hat{\nu}$ is unchanged. The multiplicative case rescales both the slope $\hat{\nu}$ and the sample mean $\overline{t_{ni}/w_i}$ by s, so the implied price elasticity of transportation supply $\overline{t_{ni}/w_i} \cdot \hat{\nu}^{-1}$ is invariant.

Calibration and counterfactuals. Additive measurement error in observed t_{ni} is absorbed exactly by the calibrated labor-per-truck requirement. From the demand-for-transportation inversion in Appendix B.5, $\hat{\varphi}_i^j = (X_{ni}^j/k_{ni}^j - t_{ni}^{\text{obs}})/w_i = \varphi_i^{j,\text{true}} - a_i/w_i$ at every observation, so the delivered cost $\hat{\varphi}_i^j w_i + t_{ni}^{\text{obs}} = \varphi_i^{j,\text{true}} w_i + t_{ni}^{\text{true}}$ is invariant. Trade shares (5), transportation demand (8), and the iceberg cost $\tau_{ni} = \varphi_i + t_{ni}/w_i$ all reproduce their true values, so the counterfactual welfare changes from Proposition 3 are unchanged. Multiplicative measurement error acts as a change in the units of t_{ni}: when accompanied by the corresponding rescaling of the structural parameters that share its units (ν, $\tilde{c}_{ni}$, f_i), it leaves dimensionless welfare percent changes unchanged.

B.3 Travel Time, Distance, and Counterfactual Road Network

Bilateral travel time and road distance are computed by ArcGIS Network Analyst on the U.S. Department of Transportation (USDOT) North American road network, across

all pairs of U.S. FAF5 regions and between U.S. regions and the five largest Canadian centres. The travel-time variable in our distance/time spline (20) is the ArcGIS time; the distance variable is the FAF5/CFAF weighted-miles measure (which also constructs the instrument IV_{ni}). The counterfactual road network for the Interstate Highway System (IHS) elimination experiment (Section 5.1) removes all IHS segments from the network and recomputes all routes. Table 9 reports the resulting changes in travel time and distance by market type; percentage changes in ArcGIS distance under network removal are applied to baseline FAF5/CFAF distances to obtain counterfactual market distances.

B.4 Value of Shipments and Trade Shares

Value of shipments in the U.S. and Canada. FAF5 reports V_{ni}^j net of freight, so we construct consumer-price values $X_{ni}^j = V_{ni}^j + t_{ni}k_{ni}^j$ with t_{ni} from Schneider and k_{ni}^j (tons) directly from FAF5. FAF5 covers U.S. internal, interstate and international flows for 16 tradable sectors; within-Canada flows are supplemented by the Canadian Freight Analysis Framework (CFAF). CFAF reports only twelve manufacturing sectors (Table 2), so we disaggregate the grouped CFAF sectors to match our NAICS aggregation. Disaggregation uses the market-clearing condition $\sum_i X_{ni}^j = \alpha^j X_n$ at the country level combined with expenditure shares α^j and the per-origin proportions from FAF5 exports to Canada; tonnages are disaggregated using the demand-for-transportation identity $X_{nn}^j/X_{nn}^{j'} = k_{nn}^j/k_{nn}^{j'}$, which is valid because per-unit shipping cost is sector-independent (see paragraph B.5).

Table 2: Grouping of Commodities Based on SCTG 2-Digit Level

Sector	Description
AGRI	Agricultural products (01, 02, 03, 04)
FOOD	Food (05, 06, 07, 08, 09)
MNRLS	Minerals (10, 11, 12, 13, 14)
COAL	Coal (15)
FUELS	Fuel oils and crude petroleum (16, 17, 18, 19)
PLCHM	Plastic and chemical products (20, 21, 22, 23, 24)
FRPAP	Forest products (25, 26, 27, 28, 29)
BMETL	Base metals and articles of base metals (31, 32, 33)
TRANS	Automobiles and other transportation equipment (36, 37)
OTHMF	Other manufactured goods (30, 34, 35, 38, 39, 40)
WASTE	Waste and scrap (41)
MISC	Miscellaneous products (42)

Trade shares. We compute bilateral sectoral trade shares directly from the consumer-price values: $\pi_{ni}^j = X_{ni}^j / \sum_i X_{ni}^j$.

B.5 Wages, Employment, and Labor per Truck

Regional employment. U.S. employment by FAF5 region is from the Bureau of Economic Analysis (BEA, Regional Economic Profiles, 2017); Canadian employment is from Statistics Canada.

Wages. Labor-market clearing (13) and trade balance imply $w_i L_i = \sum_{n,j\geq 1} X_{ni}^j + \alpha^0 X_i$, the sum of tradable and non-tradable labor income in i. We use this identity to recover $w_i = (\sum_{n,j\geq 1} X_{ni}^j + \alpha^0 X_i)/L_i$. Equivalently, $w_i = (1-\alpha^0/\alpha)^{-1} \sum_{n,j\geq 1} X_{ni}^j / L_i$ (the form used by the calibration code, which avoids the dependence of X_i on w_i).

Labor per truck requirement. Inverting the demand for transportation (8), $X_{ni}^j/k_{ni}^j = \varphi_i^j w_i + t_{ni}$, yields $\varphi_i^j = (X_{ni}^j/k_{ni}^j - t_{ni})/w_i$ at each (n,i,j). For parsimony, we calibrate φ_i at the origin level as the truck-flow-weighted average across destinations and sectors, $\varphi_i = \sum_{n,j} k_{ni}^j \varphi_i^j / k_i$ with $k_i = \sum_{n,j} k_{ni}^j$. Equivalently, aggregating the demand-for-transportation identity (8) across (n,j) and substituting labor-market clearing (paragraph B.5) yields the closed form

$$\varphi_i = \frac{(1-\alpha^0/\alpha)\, L_i \;-\; \sum_n t_{ni} k_{ni}/w_i}{k_i}.$$

B.6 Sectoral and Regional Definitions

List of sectors. The 16 tradable sectors are: Agriculture; Food Products & Beverage and Tobacco (NAICS 311–312); Textiles and Apparel/Leather (NAICS 313–316, aggregated); Wood & Paper (NAICS 321–322, aggregated); Printing (NAICS 323); Petroleum & Coal (NAICS 324); Chemicals (NAICS 325); Plastics & Rubber (NAICS 326); Nonmetallic Minerals (NAICS 327); Primary & Fabricated Metals (NAICS 331–332, aggregated); Machinery (NAICS 333); Computers & Electronics (NAICS 334); Electrical Equipment (NAICS 335); Transportation Equipment (NAICS 336); Furniture (NAICS 337); Miscellaneous (NAICS 339, absorbing Waste and Scrap). Adding the service sector gives 17.

Table 3: Description of SCTG Codes and NAICS-Aggregation to Tradable Sectors in the Model

SCTG	Goods Description	Tradable Sector
01	Animals and Fish (live)	Agriculture
02	Cereal Grains (includes seeds)	Agriculture
03	Agricultural Products	Agriculture
04	Animal Feed and Products of Animal Origin	Agriculture
05	Meat, Fish, Seafood, and Their Preparations	Food, Beverage and Tobacco
06	Milled Grain Products and Preparations	Food, Beverage and Tobacco
07	Other Prepared Food Stuffs and Fats and Oils	Food, Beverage and Tobacco
08	Alcoholic Beverages	Food, Beverage and Tobacco
09	Tobacco Products	Food, Beverage and Tobacco
10	Monumental or Building Stone	Nonmetallic Mineral
11	Natural Sands	Nonmetallic Mineral
12	Gravel and Crushed Stone	Nonmetallic Mineral
13	Other Nonmetallic Minerals	Nonmetallic Mineral
14	Metallic Ores and Concentrates	Nonmetallic Mineral
15	Coal	Petroleum and Coal
16	Crude Petroleum	Petroleum and Coal
17	Gasoline, Aviation Turbine Fuel, and Ethanol	Petroleum and Coal
18	Fuel Oils	Petroleum and Coal
19	Other Coal and Petroleum Products	Petroleum and Coal
20	Basic Chemicals	Chemical
21	Pharmaceutical Products	Chemical
22	Fertilizers	Chemical
23	Other Chemical Products and Preparations	Chemical
24	Plastics and Rubber	Chemical
25	Logs and Other Wood in the Rough	Wood and Paper
26	Wood Products	Wood and Paper
27	Pulp, Newsprint, Paper, and Paperboard	Wood and Paper
28	Paper or Paperboard Articles	Wood and Paper
29	Printed Products	Printing
30	Textiles, Leather, and Articles of Textiles or Leather	Textile, Apparel, Leather
31	Non-Metallic Mineral Products	Nonmetallic Mineral
32	Base Metal in Primary or Semi-Finished Forms	Primary and Fabricated
33	Articles of Base Metal	Primary and Fabricated
34	Machinery	Machinery
35	Electronic and Other Electrical Equipment	Electrical Equipment
36	Motorized and Other Vehicles	Transportation Equipment
37	Transportation Equipment	Transportation Equipment
38	Precision Instruments and Apparatus	Computer and Electronic
39	Furniture, Mattresses and Mattress Supports	Furniture
40	Miscellaneous Manufactured Products	Miscellaneous
41	Waste and Scrap	Miscellaneous
43	Mixed Freight	Miscellaneous
99	Commodity Unknown	Miscellaneous

Concordance table.

Table 4: FAF5 Regions

Code	FAF5 Region	State	Type
011	Birmingham-Hoover-Talladega	AL	C
012	Mobile-Daphne-Fairhope	AL	C
019	Remainder of Alabama	AL	R
020	Alaska	AK	S
041	Phoenix-Mesa-Scottsdale	AZ	C
042	Tucson-Nogales	AZ	C
049	Remainder of Arizona	AZ	R
050	Arkansas	AR	S
061	Los Angeles-Long Beach	CA	C
062	Sacramento-Roseville	CA	C
063	San Diego-Carlsbad	CA	C
064	San Jose-San Francisco-Oakland	CA	C
065	Fresno-Madera	CA	C
069	Remainder of California	CA	R
081	Denver-Aurora	CO	C
089	Remainder of Colorado	CO	R
091	Hartford-West Hartford-East Hartford	CT	C
092	New York-Newark, NY-NJ-CT-PA	CT	C
099	Remainder of Connecticut	CT	R
101	Philadelphia-Reading-Camden,PA, NJ, DE, MD	DE	C
109	Remainder of Delaware	DE	R
111	Washington-Arlington-Alexandria,DC-VA-MD-WV	DC	C
121	Jacksonville-St. Marys-Palatka, FL-GA	FL	C
122	Miami-Fort Lauderdale-Port St. Lucie	FL	C
123	Orlando-Deltona-Daytona Beach	FL	C
124	Tampa-St. Petersburg-Clearwater	FL	C
129	Remainder of Florida	FL	R
131	Atlanta-Athens-Clarke County-Sandy Springs	GA	C
132	Savannah-Hinesville-Statesboro	GA	C
139	Remainder of Georgia	GA	R
151	Urban Honolulu	HI	C
159	Remainder of Hawaii	HI	R
160	Idaho	ID	S
171	Chicago-Naperville, IL-IN-WI	IL	C
172	St. Louis-St. Charles-Farmington, MO-IL	IL	C
179	Remainder of Illinois	IL	R
181	Chicago-Naperville, IL-IN-WI	IN	C
182	Indianapolis-Carmel-Muncie	IN	C
183	Fort Wayne-Huntington-Auburn	IN	C
189	Remainder of Indiana	IN	R
190	Iowa	IA	S
201	Kansas City-Overland Park-Kansas City, MO-KS	KS	C
202	Wichita-Arkansas City-Winfield	KS	C
209	Remainder of Kansas	KS	R
211	Cincinnati-Wilmington-Maysville, OH-KY-IN	KY	C
212	Louisville/Jefferson County-Elizabethtown-Madison, KY-IN	KY	C
219	Remainder of Kentucky	KY	R
221	Baton Rouge	LA	C
222	Lake Charles-Jennings	LA	C

Code	FAF5 Region	State	Type
223	New Orleans-Metairie-Hammond, LA-MS	LA	C
229	Remainder of Louisiana	LA	R
230	Maine	ME	S
241	Baltimore-Columbia-Towson	MD	C
242	Washington-Arlington-Alexandria, DC-VA-MD-WV	MD	C
249	Remainder of Maryland	MD	R
251	Boston-Worcester-Providence, MA-RI-NH-CT	MA	C
259	Remainder of Massachusetts	MA	R
261	Detroit-Warren-Ann Arbor	MI	C
262	Grand Rapids-Wyoming-Muskegon	MI	C
269	Remainder of Michigan	MI	R
271	Minneapolis-St. Paul, MN-WI	MN	C
279	Remainder of Minnesota	MN	R
280	Mississippi	MS	S
291	Kansas City-Overland Park-Kansas City, MO-KS	MO	C
292	St. Louis-St. Charles-Farmington, MO-IL	MO	C
299	Remainder of Missouri	MO	R
300	Montana	MT	S
311	Omaha-Council Bluffs-Fremont, NE-IA	NE	C
319	Remainder of Nebraska	NE	R
321	Las Vegas-Henderson, NV-AZ	NV	C
329	Remainder of Nevada	NV	R
331	Boston-Worcester-Providence, MA-RI-NH-CT	NH	C
339	Remainder of New Hampshire	NH	R
341	New York-Newark, NY-NJ-CT-PA	NJ	C
342	Philadelphia-Reading-Camden, PA-NJ-DE-MD	NJ	C
350	New Mexico	NM	S
361	Albany-Schenectady	NY	C
362	Buffalo-Cheektowaga	NY	C
363	New York-Newark, NY-NJ-CT-PA	NY	C
364	Rochester-Batavia-Seneca Falls	NY	C
369	Remainder of New York	NY	R
371	Charlotte-Concord, NC-SC	NC	C
372	Greensboro-Winston-Salem-High Point	NC	C
373	Raleigh-Durham-Chapel Hill	NC	C
379	Remainder of North Carolina	NC	R
380	North Dakota	ND	S
391	Cincinnati-Wilmington-Maysville, OH-KY-IN	OH	C
392	Cleveland-Akron-Canton	OH	C
393	Columbus-Marion-Zanesville	OH	C
394	Dayton-Springfield-Sidney	OH	C
399	Remainder of Ohio	OH	R
401	Oklahoma City-Shawnee	OK	C
402	Tulsa-Muskogee-Bartlesville	OK	C
409	Remainder of Oklahoma	OK	R
411	Portland-Vancouver-Salem, OR-WA	OR	C
419	Remainder of Oregon	OR	R

Code	FAF5 Region	State	Type
421	Philadelphia-Reading-Camden, PA-NJ-DE-MD	PA	C
422	Pittsburgh-New Castle-Weirton, PA-OH-WV	PA	C
423	New York-Newark, PA-NY-NJ-CT	PA	C
429	Remainder of Pennsylvania	PA	R
441	Boston-Worcester-Providence, MA-RI-NH-CT	RI	C
451	Charleston-North Charleston	SC	C
452	Greenville-Spartanburg-Anderson	SC	C
459	Remainder of South Carolina	SC	R
460	South Dakota	SD	S
471	Memphis-Forrest City, TN-MS-AR	TN	C
472	Nashville-Davidson-Murfreesboro	TN	C
473	Knoxville-Morristown-Sevierville	TN	C
479	Remainder of Tennessee	TN	R
481	Austin-Round Rock	TX	C
482	Beaumont-Port Arthur	TX	C
483	Corpus Christi-Kingsville-Alice	TX	C
484	Dallas-Fort Worth, TX-OK	TX	C
485	El Paso-Las Cruces, TX-NM	TX	C
486	Houston-The Woodlands	TX	C
487	Laredo	TX	C
488	San Antonio-New Braunfels	TX	C
489	Remainder of Texas	TX	R
491	Salt Lake City-Provo-Orem	UT	C
499	Remainder of Utah	UT	R
500	Vermont	VT	S
511	Richmond	VA	C
512	Virginia Beach-Norfolk, VA-NC	VA	C
513	Washington-Arlington-Alexandria, VA-DC-MD-WV	VA	C
519	Remainder of Virginia	VA	R
531	Seattle-Tacoma	WA	C
532	Portland-Vancouver-Salem, WA-OR	WA	C
539	Remainder of Washington	WA	R
540	West Virginia	WV	S
551	Milwaukee-Racine-Waukesha	WI	C
559	Remainder of Wisconsin	WI	R
560	Wyoming	WY	S
801	Canada		

Note: Type codes: C = Combined Statistical Area (CSA), M = Metropolitan Statistical Area (MSA), R = Rest of State (everything not in a CSA or MSA), S = State without a CSA or MSA, SM = Whole state is part of MSA.

FAF5 regions.

B.7 Sectoral Expenditure Shares, Land Endowments, and Productivity Scale Parameters

Sectoral expenditure shares. Sectoral expenditure shares follow Caliendo et al. (2018):

$$\alpha^j = \frac{\text{GDP}^j + M^j - E^j}{\text{GDP} + \sum_j (M^j - E^j)},$$

with U.S. sectoral trade flows from FAF5 and GDP from the BEA; Canadian data from Statistics Canada. Trade elasticities θ^j are taken from Caliendo et al. (2018), with Agriculture from Caliendo and Parro (2015). Resulting values appear in Table 5.

Table 5: Dispersion of Productivities and Share of Final Expenditure by Sector

Sector	θ^j	Canada α^j	U.S. α^j
Tradable goods $(j = 1, \ldots, J)$			
Agriculture	8.11	0.0105	0.0067
Food, Beverage, Tobacco	2.55	0.0141	0.0150
Textile, Apparel, Leather	9.46	0.0000	0.0050
Wood and Paper	9.07	0.0023	0.0020
Printing	51.08	0.0043	0.0095
Petroleum and Coal	4.75	0.0178	0.0192
Chemical Products	1.66	0.0066	0.0040
Plastics and Rubber	2.76	0.0045	0.0029
Nonmetallic Mineral	6.78	0.0112	0.0137
Primary and Fabricated Metal	5.56	0.0080	0.0076
Machinery	1.52	0.0158	0.0090
Computer and Electronic	12.79	0.0176	0.0139
Electrical Equipment	10.6	0.0087	0.0156
Transportation Equipment	1.01	0.0248	0.0197
Furniture	5.0	0.0030	0.0041
Miscellaneous	5.0	0.0075	0.0050
$\sum_{j=1}^{J} \alpha^j$		0.1566	0.1530
Non-tradable goods $(j = 0)$			
α^0		0.5934	0.5970
Residential land			
$1 - \alpha$		0.2500	0.2500
Total		1.0000	1.0000

Note: Trade elasticities θ^j from Caliendo et al. (2018), except Agriculture from Caliendo and Parro (2015). The table reports the three components of aggregate expenditure that sum to one. Tradable-goods expenditure shares α^j for $j = 1, \ldots, J$ follow the Caliendo et al. procedure using U.S. GDP and FAF5 trade flows (Statistics Canada for Canada), as described in Appendix B.7. The residential-land share $1 - \alpha = 0.25$ is taken from Redding (2016). The non-tradable share α^0 is then obtained residually as $\alpha^0 = \alpha - \sum_{j=1}^{J} \alpha^j$ so that total expenditure sums to one.

Relative land area. We invert the population mobility condition (15) for relative land endowments. Taking the ratio at locations n and 1, $L_n/L_1 = (H_n/H_1)(P_1/P_n)^{\alpha/(1-\alpha)}(w_n/w_1)^{\alpha/(1-\alpha)}$, we solve for H_n/H_1 given observed L_n, w_n, and the relative price index P_1/P_n. Sectoral indices for $j \geq 1$ follow from (6) after substituting the demand inversion $\varphi_i^j w_i + t_{ni} = X_{ni}^j/k_{ni}^j$; the non-tradable price is $P_n^0 = w_n/A_n^0$; aggregation $P_n = \prod_{j=0}^{J}(P_n^j)^{\alpha^j/\alpha}$ then expresses P_1/P_n in terms of observables $(X_{ni}^j, k_{ni}^j, w_n)$ and calibrated primitives $(A_i^j, \theta^j, \alpha^j, \alpha^0)$, with α^0 entering through the non-tradable component.

Productivity scale parameters. The Fréchet productivity scale parameters A_i^j are recovered from the trade-share equation (5), given the calibrated input costs $\varphi_i w_i + t_{ni}$ (paragraphs B.5 and B.5), the trade elasticities θ^j from Caliendo et al. (2018) and Caliendo and Parro (2015), and observed bilateral trade shares π_{ni}^j from FAF5/CFAF.

The trade-share equation does not invert pointwise: A_i^j enters both the numerator of (5) and the multilateral-resistance denominator $\Phi_n^j = \sum_s A_s^j(\varphi_s w_s + t_{ns})^{-\theta^j}$, so the parameters $\{A_i^j\}_{i=1}^N$ in each sector are determined jointly. We normalize $A_1^j = 1$ and pin the remaining $N-1$ parameters down by matching the sum of trade shares from each origin across destinations to its model-implied counterpart: for each (i, j),

$$\sum_n \pi_{ni}^j \;=\; A_i^j \sum_n \frac{(\varphi_i w_i + t_{ni})^{-\theta^j}}{\Phi_n^j(A_1^j, \ldots, A_N^j)}.$$

This is a fixed-point system in $\{A_i^j\}_i$ at each sector j, coupled across origins through Φ_n^j. We solve it numerically by iteration: at each pass A_i^j is updated as the ratio of the LHS (data) to the inner sum (model evaluated with the current Φ_n^j), and Φ_n^j is recomputed from the updated $\{A_i^j\}$, until convergence.

B.8 Instrumental Variable: Relevance and Validity

Our IV is constructed to shift the demand for transportation by influencing the destination's multilateral resistance Φ_n^j in the structural gravity equation

$$\pi_{ni}^j = \frac{Y_i^j}{\Omega_i^j} \cdot \frac{\phi_{ni}^j}{\Phi_n^j}, \qquad \phi_{ni}^j = (\varphi_i w_i + t_{ni})^{-\theta^j}, \tag{A.41}$$

in the sense of Head and Mayer (2014), with $Y_i^j = \sum_n X_{ni}^j$ and $\Omega_i^j = \sum_\ell X_\ell^j \phi_{\ell i}^j / \Phi_\ell^j$. Writing the demand for transportation as $\log k_{ni} = \log X_n - \log(\varphi_i w_i + t_{ni}) + \log \sum_j \alpha^j \, (Y_i^j/\Omega_i^j) \, (\phi_{ni}^j/\Phi_n^j)$, and Taylor-expanding $\log \Phi_n^j$ to first order around a symmetric equilibrium (all locations identical, all bilateral transportation prices equal to a common $\bar{t}$),

$\log \Phi_n^j \approx \text{const} - \frac{\theta^j}{\varphi w + \bar{t}} \frac{1}{N} \sum_\ell (t_{n\ell} - \bar{t})$, aggregating across sectors and absorbing origin- and destination-specific terms yields $\log k_{ni} \approx \text{const} + \tilde{\beta} \sum_{\ell \neq i} t_{n\ell}$ with $\tilde{\beta} > 0$. Since $t_{n\ell}$ is endogenous, we replace it with the geographic analogue $\text{dist}_{n\ell}$—the deterministic, exogenous component of bilateral transportation prices—yielding the instrument $IV_{ni} = \sum_{\ell \neq i} \text{dist}_{n\ell}$ in (21).

The exclusion restriction requires IV_{ni} uncorrelated with unobserved fundamental costs u_{ni} conditional on the controls in (19). Because the estimating equation already includes a flexible spline in bilateral dist_{ni} and time_{ni}, plus border dummies and origin fixed effects, the identifying variation in IV_{ni} comes from the geographic position of n

relative to third-party locations $\ell \neq i$—not from bilateral characteristics of the (n, i) market. The exclusion restriction fails only if bilateral unobservables u_{ni} are systematically correlated with the remoteness of n from third parties, conditional on the (n, i) controls; we view this as implausible. Subsection B.10 adds destination-specific infrastructure controls directly, finding that $\hat{\nu}$ moves *upward*—opposite to the direction predicted by such a violation.

B.9 Identification of Fundamental Costs

Estimation of (19) identifies within-origin variation in fundamental costs. The spline (20) omits an intercept, implicitly normalising the origin-specific level of c_{ni} to zero (equivalently, choose $\bar{c}_i = 0$; any other choice gives the same equilibrium by Lemma 2 below). We show here that this normalisation is inconsequential: the equilibrium depends on c_{ni} and f_i only through their sum, so we set $c_{ni} = \tilde{c}_{ni}$ and pin $c_{ni} + f_i$ down via the origin-specific free entry condition. Calibration and counterfactual outputs are invariant.

Lemma 2 (Observational equivalence)**.** *For any origin-specific constant $\bar{c}_i$, the reparameterisation $c_{ni} \to c_{ni} + \bar{c}_i$, $f_i \to f_i - \bar{c}_i$ leaves all equilibrium outcomes unchanged.*

Proof. Only (9) and (10) involve c_{ni} and f_i. In (9), the shift multiplies numerator and denominator by $\exp(-\bar{c}_i/\nu)$ and cancels. In (10), both sides shift by $-w_i\bar{c}_i$. The remaining equilibrium equations—trade shares, price indices, demand for transportation, market clearing, labor income, land market, population mobility—do not contain c_{ni} or f_i. □

Calibration. Given ν and $\tilde{c}_{ni}$, the free-entry condition pins f_i down once $c_{ni} = \tilde{c}_{ni}$ is imposed; using any other normalisation $(\tilde{c}_{ni} + \bar{c}_i, f_i - \bar{c}_i)$ leaves the sum unchanged, and by Lemma 2 the equilibrium is invariant. The remaining calibrated parameters φ_i, H_i, A_i^j are recovered from (8), (15), (5) using observables and primitives that do not involve c_{ni} or f_i.

Counterfactual exercises. Each counterfactual shock Δc_{ni} does not depend on $\bar{c}_i$, and by Lemma 2 the equilibrium system that processes the shock is itself invariant. For the IHS elimination, $\Delta c_{ni} = \tilde{c}_{ni}^{CF} - \tilde{c}_{ni}$ is a difference of spline evaluations at identified coefficients; for interstate-regulation harmonisation, $\Delta c_{ni} = -\hat{\delta}_{\text{STATE\_border}} \cdot \text{STATE\_border}_{ni}$, a coefficient times an indicator; for the border closure, international transportation markets are removed entirely. The autonomous-trucks shock $\Delta c_{ni} = -0.45 \cdot \tilde{c}_{ni}$ requires additional care: since $\tilde{c}_{ni}$ has no intercept (equation (20)), it contains no level-normalisation constant. Economically, the autonomous-trucks shock reduces the distance, time, and border *gradients* of shipping costs by 45%—consistent with driver-labour savings, extended daily

range, and reduced fuel use being proportional to marginal per-mile and per-hour components.

B.10 Robustness

Omitted destination variables: data. $IV_{ni} = \sum_{\ell \neq i} \text{dist}_{n\ell}$ varies primarily across destinations. Destinations geographically remote from most origins receive high values, and they may also have high unobserved fundamental costs (poor local roads, thin driver labour markets). Destination fixed effects are infeasible (see §4.2); we therefore add destination-specific *controls*—employment plus 2017 infrastructure measures from the National Bridge Inventory (NBI) and the Highway Performance Monitoring System (HPMS)—to the baseline 2SLS. Destination controls: (i) L_n employment, from the baseline dataset. We include L_n as a proxy for destination market scale. Under the model's population-mobility condition, L_n is ultimately an equilibrium outcome and hence we excluded it from our baseline specification in Table 3. However, population is likely to adjust more slowly than wages and expenditure to transportation-cost variation, so L_n is a reasonable—if imperfect—short-run proxy. We exclude X_n and w_n as bad controls, since they adjust jointly with transportation costs. (ii) NBI, 128 destinations: average bridge condition (0–9 deck/superstructure/substructure mean), share structurally deficient (min rating ≤ 4), average bridge age, aggregated from 612,677 records via county-to-FAF5 concordance. (iii) HPMS, 127 destinations (DC excluded): average International Roughness Index (IRI, in/mi), share poor pavement (IRI$>$ 170), log total lane-miles, share National Highway System (NHS), from 6.8M road segments via the same concordance. Summary statistics in Table 6.

Source	Variable	Mean	Std. Dev.	Min	Max
Baseline	L_n (000s)	1,276	1,843	30	12,099
NBI	Avg. bridge condition (0–9)	6.58	0.35	5.73	7.81
	Share deficient (%)	8.4	6.1	0.0	29.5
	Avg. bridge age (yrs)	44.0	7.4	24.0	64.7
HPMS	Avg. IRI (in/mi)	53.9	35.5	0.0	217.4
	Share poor pavement (%)	8	9	0	64
	Total lane-miles (000s)	19.2	31.8	0.03	221.7
	Share NHS (%)	25	10	0	49

Table 6: Destination-level controls: summary statistics. Employment $N = 129$; NBI $N = 128$ (Canada excluded); HPMS $N = 127$ (Canada and DC excluded). Detailed definitions of each NBI/HPMS variable follow the FHWA standard manuals.

Omitted destination variables: regression results. Table 7 adds the controls one family at a time. Column (1) reproduces the baseline ($\hat{\nu} = .103$). Column (2) adds $\log L_n$: $\hat{\nu} = .167$. Columns (3)–(4) add HPMS and NBI controls separately: $\hat{\nu} = .121$ and .140,

both with first-stage $F > 92$. Column (5) combines all controls: $\hat{\nu} = .227$. The informative columns for the omitted-variable concern are (3) and (4): they add infrastructure-quality controls directly without re-introducing the $\log L_n$ channel that motivated L_n's exclusion from the baseline (column (5) combines all controls and is harder to interpret for the same reason). Both move $\hat{\nu}$ *upward*—opposite to the direction predicted by the omitted-variable story—so the baseline estimate is, if anything, conservative.

Table 7: 2SLS estimation with destination-level controls.

	(1) Baseline	(2) $+L_n$	(3) +HPMS	(4) +NBI	(5) All
Truck share: $\log(k_{ni}/k_i)$	$.103^{***}$	$.167^{***}$	$.121^{***}$	$.140^{***}$	$.227^{***}$
	(.020)	(.035)	(.025)	(.023)	(.047)
US–CAN border	$.126^{**}$	$.772^{***}$	$.308^{***}$	$.350^{***}$	$.509^{***}$
	(.051)	(.086)	(.064)	(.064)	(.095)
STATE border	$.164^{***}$	$.251^{***}$	$.174^{***}$	$.202^{***}$	$.313^{***}$
	(.040)	(.050)	(.046)	(.044)	(.064)
Origin FE, distance/time splines	Y	Y	Y	Y	Y
$\log L_n$ / HPMS / NBI		$\log L_n$	HPMS	NBI	All
N	16,498	16,498	16,241	16,369	16,241
First-stage F	143.72	53.40	92.41	134.28	47.33

All columns estimate (19) by 2SLS with origin FEs, instrumented by IV_{ni}. State-pair clustered SEs in parentheses. Columns (3) and (5) drop Canadian markets (HPMS unavailable); Column (4) drops Canada (NBI unavailable). $^{*}p < .10$, $^{**}p < .05$, $^{***}p < .01$.

Standard errors. Table 8 reports $\hat{\nu}$ under alternative specifications, varying one dimension at a time: clustering of standard errors, construction of the instrument, functional form of fundamental-cost controls, and estimation sample. The point estimate is invariant to the variance estimator; only SEs change.

Destination clustering (row 3) and Conley (1999) spatial-HAC at 60, 90, and 150 miles applied to destination coordinates (rows 5–7; a smooth-decay analog of destination clustering) drop the partial F between 9.34 and 11.73, below the Stock and Yogo (2005) 10% critical value of 16.38. The Stock–Yogo threshold itself is a statement about Wald reliability: when F falls below it, the conventional nominal-5% Wald can have actual size in excess of 10%. The drop in F does not by itself prevent inference, however. The Anderson and Rubin (1949) test sidesteps this by construction — it has correct size at any first-stage strength — and its 95% confidence interval is the appropriate inferential output. Rows (20)–(21) report weak-IV-robust AR 95% CIs for ν, computed via the `weakiv` package (Finlay et al., 2014). Both AR intervals reject $\nu = 0$ at 5%; the destination-clustered AR conclusion also covers the Conley HAC specifications by

similarity, since their SE and F statistics are nearly identical.

Reporting AR alongside the high-F baseline (row 20 vs. row 1) is also informative. Keane and Neal (2024) document that the 2SLS t-test exhibits a power asymmetry — standard errors are spuriously small in samples where $\hat{\beta}_{2SLS}$ is shifted toward OLS — that persists at first-stage F values well above conventional weak-IV thresholds, with AR overturning t-test conclusions in 24% of 49 IV papers they review in the AER (2011–2023). They recommend AR as the default IV inference procedure regardless of first-stage strength. The close agreement between Wald and AR under state-pair clustering shows the high-F baseline result is not a finite-sample artifact.

Reduced form. The direct OLS regression of t_{ni}/w_i on IV_{ni} (with all controls) gives $t = 6.62$: the instrument moves the outcome in the expected direction.

Alternative instruments. Replacing the distance-based IV with a time-based analog gives $\hat{\nu} = .097$; using ArcMap (rather than FAF5 weighted-miles) distances gives .089; log-transformed IV gives .135. First-stage $F > 118$ in all three. The narrow range across constructions reflects near-perfect correlation ($\rho = .99$) between bilateral distance and time.

Functional form. Quadratic-in-(dist, time) controls give $\hat{\nu} = .101$; distance-spline only .100; time-spline only .108 (the distance-only and time-only estimates are nearly identical, consistent with the high distance–time correlation). Stability here is expected: ν is identified from IV-driven demand shifts, not the parameterisation of the controls.

Sample restrictions. Dropping Canada (257 markets) gives .104; dropping internal markets ($i = n$, 129 markets) gives .102; trimming $p1$–$p99$ of distance gives .107; trimming $p1$–$p99$ of price gives .086; trimming $p1$–$p99$ of tons gives .110.

Summary. Across the 18 2SLS specifications in rows (1)–(18) of Table 8, $\hat{\nu}$ ranges from 0.086 to 0.135, with implied price elasticity of transportation supply $(\overline{t_{ni}/w_i})\hat{\nu}^{-1}$ between 6.1 and 9.5, around the baseline of 7.9.

Table 8: Robustness of $\hat{\nu}$.

	Specification	$\hat{\nu}$	SE	First-stage F	N
Baseline					
(1)	Spline, state-pair cluster	0.103***	0.020	143.72	16,498
Alternative clustering					
(2)	Origin cluster	0.103***	0.028	118.79	16,498
(3)	Destination cluster	0.103*	0.055	9.34	16,498
(4)	Robust HC1 (no cluster)	0.103***	0.009	357.33	16,498
(5)	Conley spatial HAC (60 mi)	0.103*	0.055	10.05	16,498
(6)	Conley spatial HAC (90 mi)	0.103*	0.055	11.27	16,498
(7)	Conley spatial HAC (150 mi)	0.103*	0.058	11.73	16,498
Alternative instruments					
(8)	Time-based IV	0.097***	0.019	152.50	16,498
(9)	ArcMap distance IV	0.089***	0.018	157.30	16,498
(10)	Log-transformed IV	0.135***	0.022	118.18	16,498
Functional form of controls					
(11)	Quadratic	0.101***	0.019	139.93	16,498
(12)	Distance spline only	0.100***	0.020	142.43	16,498
(13)	Time spline only	0.108***	0.021	121.87	16,498
Sample restrictions					
(14)	U.S.-only (drop CA markets)	0.104***	0.020	144.92	16,241
(15)	Drop internal markets	0.102***	0.019	178.05	16,369
(16)	Trimmed (p1–p99 distance)	0.107***	0.020	156.46	16,169
(17)	Trimmed (p1–p99 price)	0.086***	0.017	175.24	16,172
(18)	Trimmed (p1–p99 tons)	0.110***	0.020	193.29	16,169
Reduced form					
(19)	t_{ni}/w_i on IV_{ni}	$t = 6.62$			16,498
Anderson–Rubin weak-IV-robust inference					
(20)	AR 95% CI, state-pair cluster	[0.068, 0.146]		$p < 0.001$	16,498
(21)	AR 95% CI, destination cluster	[0.035, 0.451]		$p = 0.005$	16,498

Rows (1)–(18) are 2SLS of (19) with origin FEs; row (19) is the reduced-form t-stat of IV_{ni} on t_{ni}/w_i. Rows (20)–(21) are Anderson and Rubin (1949) weak-IV-robust 95% confidence intervals for ν (computed via the Stata `weakiv` package, Finlay et al., 2014); for these rows we report the AR p-value at $\nu = 0$. SE at state-pair cluster except where noted. Rows (5)–(7) are Conley (1999) spatial HAC with Bartlett kernel on destination coordinates, as a smooth-decay analog of destination clustering. First-stage F on the excluded IV; Stock and Yogo (2005) 10% critical value is 16.38. $^{*}p < .10$, $^{**}p < .05$, $^{***}p < .01$.

C Counterfactual Exercises: Data and Additional Results

This appendix documents the additional inputs required by the four counterfactual experiments in Section 5 and reports supplementary results that complement Figures 5–8 and Table 5 of the main text. Subsection C.1 reports counterfactual travel time and distance under the IHS-removal experiment (Section 5.1); Subsections C.2 and C.3 document the regulatory differences that motivate, respectively, the interstate-regulation harmonization (Section 5.2) and U.S.–Canada border-closure (Section 5.3) experiments. Subsections C.4–C.6 report supplementary outputs across all four counterfactuals: the iceberg-cost shock by market type, the per-component decomposition of supply and demand shifters, and the spatial distribution of real-income effects.

C.1 Counterfactual Data for the Interstate Highway System

Table 9 reports travel time and distance before and after IHS elimination, by market type. Counterfactual distances and times are computed on the North American road network excluding all Interstate segments (Subsection B.3).

Table 9: Travel Time and Distance Before/After IHS Removal by Market Type

	Market Type	Time (hours)		% Change	Distance (miles)		% Change
		Before	After		Before	After	
U.S.	Internal	0.61	0.61	0	56	56	0
	Intrastate	3.55	4.25	19.70	222.29	237.98	7.06
	Interstate	18.72	23.53	25.74	1,219.19	1,308.64	7.34
	International	17.91	21.66	20.92	1,149.00	1,197.95	4.26
Canada	Internal	0.36	0.36	0	251	251	0

Note: Average travel time and distance by market type before and after the elimination of the Interstate Highway System (IHS). Travel time and distance are computed from the ArcMap road network (see Appendix B.3).

C.2 Interstate Trucking Regulations

The state-border effect estimated on interstate transportation markets in Section 4.2 reflects the body of regulations that govern, tax, or constrain motor-carrier operations across state lines. We use the term *interstate trucking regulations* broadly: it encompasses both (i) heterogeneous state-level regulations that bind on interstate trucking through the requirement to comply with each traversed state's rules and (ii) the multi-state administrative regime—a combination of federal regulations and federally-mandated interstate

compacts—that activates whenever a carrier operates across a state line. The first set generates a cost wedge through cross-state *heterogeneity*: uniform state regulations, however strict, would not raise the cost of interstate relative to intrastate shipments. The second generates a cost wedge through *regime activation*: even if every state's regulations were identical, an interstate operation triggers compliance burdens that intrastate-only carriers can avoid altogether. Table 10 summarises the main channels of both.

Dimension	Regulation	Mechanism of interstate cost wedge
Gross vehicle weight	Federal Interstate floor at 80,000 lbs (23 U.S.C. §127); states set higher limits on state highways	MI permits up to 164,000 lbs on certain state highways (11-axle); NV ∼129,000 lbs on designated routes; 12+ additional states allow >80,000 lbs on permitted routes. Interstate carriers must reduce payload at the lower-limit state border.
Longer Combination Vehicles (LCVs)	ISTEA 1991 freeze: pre-1991 states may continue LCV operations, others prohibited	23 states (mostly West/Midwest) permit triple-trailer configurations; most NE/SE states and CA prohibit entirely. LCV configurations legal at origin must be broken down into standard semitrailers when crossing into a prohibiting state.
Oversize/overweight (OS/OW) permits	State-issued; required for any load exceeding state limits	Single-trip permit fees from $5 (FL) to $97 (PA); overweight surcharges $0.12–$1.00/mi; escort requirements range from 1 (TX) to 4 incl. police (NY) for >16-ft loads. A cross-country shipment may require separate permits in every state traversed.
Multi-state administrative regime	Federal regulations (49 CFR) and federally-mandated interstate compacts (IFTA, IRP)	Activates upon any interstate operation; intrastate-only carriers exempt. (i) IFTA: quarterly fuel-tax returns apportioning miles and fuel use across operating jurisdictions; (ii) IRP: apportioned vehicle registration; (iii) federal financial responsibility (49 CFR 387): $750K BI/PD minimum ($1M–$5M hazmat) vs. $300K–$750K state minima for intrastate-only; (iv) FMCSA safety regime (49 CFR 382, 391, 395, 396): USDOT number, hours-of-service, driver qualification, drug/alcohol testing, ELD, CSA scoring.

Sources. Gross vehicle weight: FHWA STWL Compilation. LCVs: FHWA; GAO RCED-94-106. OS/OW permits: State DOT guides. Multi-state administrative regime: 49 CFR; IFTA, Inc.; AAMVA. *Abbreviations.* AAMVA, American Association of Motor Vehicle Administrators; BI/PD, bodily-injury and property-damage liability; CSA, Compliance, Safety, Accountability (FMCSA's safety-scoring program); ELD, electronic logging device; FHWA, Federal Highway Administration; FMCSA, Federal Motor Carrier Safety Administration; GAO, U.S. Government Accountability Office; ISTEA, Intermodal Surface Transportation Efficiency Act of 1991; USDOT, U.S. Department of Transportation.

Table 10: Selected U.S. interstate trucking regulations, 2017.

State regulations

The first three rows of Table 10 reflect federal legislation that set minimum standards while preserving state variation along three dimensions: weight limits, longer combination

vehicles, and oversize/overweight permitting. The Surface Transportation Assistance Act of 1982 (STAA) established federal minimum trailer standards on the National Network but grandfathered pre-existing state weight limits, allowing states with higher pre-1982 caps to retain them. The Intermodal Surface Transportation Efficiency Act of 1991 (ISTEA) froze LCV operations at then-existing state allowances: states that permitted LCVs before June 1, 1991 may continue, while states that did not are barred from introducing them. Subsequent reauthorisations—the Moving Ahead for Progress in the 21st Century Act of 2012 (MAP-21), the Fixing America's Surface Transportation Act of 2015 (FAST Act), and the Infrastructure Investment and Jobs Act of 2021 (IIJA)—funded infrastructure and mandated comprehensive size-and-weight studies (including the FHWA *Comprehensive Truck Size and Weight Limits Study* delivered to Congress in 2016) but did not alter the federal weight limits or the LCV freeze. We discuss each of the three regulatory dimensions in turn.

Weight limits. Weight-limit heterogeneity is one of the most direct sources of payload-related cost variation across states. Under STAA grandfather clauses, Michigan permits up to 164,000 lbs on certain state highways using an 11-axle "Michigan train" configuration, more than double the federal 80,000 lb Interstate cap; Nevada permits up to roughly 129,000 lbs on designated routes; and a dozen additional western and midwestern states (including Indiana, Iowa, Kansas, Missouri, Montana, Nebraska, North Dakota, Oklahoma, Oregon, South Dakota, Washington, and Wisconsin) allow weights above 80,000 lbs on designated non-Interstate routes or under permit. A Michigan-based carrier loading 130,000 lbs of aggregate to a destination 200 miles away within Michigan can do so under state law; an interstate route of identical distance and travel time to a destination in Ohio is subject to the federal 80,000 lb cap, forcing either a 38% payload reduction or an Ohio overweight permit with associated fees and escort requirements.

Longer combination vehicles. The LCV patchwork is similarly heterogeneous: roughly 23 mostly western and midwestern states permit triple-trailer or other longer combination vehicle configurations under ISTEA's grandfather provisions, while most northeastern, southeastern, and West-Coast states (including California) prohibit them entirely. An Idaho-based carrier running triple 28-foot trailers on an intrastate route must break the triple down into standard semitrailers near the border to enter California on an interstate route of identical distance and travel time, requiring additional tractors, drivers, staging space at a terminal or truck stop near the border, and the labor needed to redistribute cargo across the new configurations.

Oversize/overweight permitting. OS/OW permitting adds a third layer of cross-state heterogeneity that affects loads exceeding standard limits, which is a small share of

shipments overall but a large share of construction, energy, and agricultural transport. Single-trip permit fees vary by more than an order of magnitude across states: Florida charges $5 for a 7-day oversize permit, Colorado $15, California $16, while Pennsylvania charges $46 for loads under 14 ft wide rising to $97 above (with an additional $37 PA Turnpike fee plus $0.24 per ton-mile over 80,000 lbs), and Texas charges $60 plus $0.12 per mile plus $25 per foot of width above 14 ft. Escort requirements vary similarly: a 15-foot-wide load requires one private escort in Texas, two in California (with California Highway Patrol escort over 16 ft), one to two in Pennsylvania, and a four-vehicle escort including police in New York. Operating-hour and holiday windows compound the heterogeneity: Pennsylvania and California both prohibit Sunday OS/OW travel year-round; Minnesota blocks OS/OW operations on "Fishing Opener Weekend" (May) and during summer Friday/Sunday-evening curfews; and processing times for superload permits range from minutes (Texas's TxPROS self-issuance system) to two or three weeks (Colorado's superload review). A complex cross-country OS/OW move can require ten or more state permits, costing $1,000–$5,000 in fees alone before counting escort, scheduling, and processing-delay costs.

Multi-state administrative regime

The four channels in the bottom row of Table 10 are triggered the moment a motor carrier transports property across a state line: an interstate carrier is subject to all four; an intrastate-only carrier (whose vehicles never leave the home state) avoids them altogether. They generate cost wedges through two distinct mechanisms. The IRP channels *state-level trucking-regulation heterogeneity* through an apportionment regime: each member jurisdiction sets its own annual per-vehicle commercial-registration fee independently, and the carrier's annual IRP liability is the mileage-weighted sum of these state-set fees ($\sum_j m_j F_j$, with m_j the carrier's mileage share in jurisdiction j and F_j that jurisdiction's per-vehicle fee); under uniform fees no substantive IRP wedge would arise, leaving only the administrative compliance burden of mileage reporting and annual apportionment recalculation. The remaining three channels generate wedges through *regime activation* that survive even under identical state-level rules. IFTA imposes a quarterly fuel-tax-apportionment compliance regime—mileage and fuel tracking by jurisdiction, periodic filing, and audit risk.[6] The federal financial-responsibility minima impose a $750,000 bodily-injury and property-damage (BI/PD) floor ($1M–$5M for hazmat) on every interstate motor carrier, supplanting the (typically lower) home-state intrastate minimum and raising annual insurance premia. The FMCSA safety regime imposes USDOT registration, federal hours-of-service, driver qualification files, drug and alcohol testing, the ELD

[6]Cross-state variation in per-gallon fuel-tax rates does affect an interstate carrier's quarterly IFTA liability, but those rates are general state tax policy applying to all motor vehicles rather than trucking-specific regulation, so we do not classify them as trucking-regulation heterogeneity.

mandate, and periodic vehicle inspections on every interstate motor carrier, supplanting the (often narrower) state-law safety regime with its various intrastate exemptions; weigh-station inspections at any state's facility fold into a nationally-aggregated CSA score that shippers and insurers use to price the carrier. Together, the four channels generate per-trip or per-vehicle costs on cross-state operations that have no intrastate-only counterpart, contributing to the estimated state-border premium.

C.3 U.S.–Canada Cross-Border Trucking Costs

Crossing the U.S.–Canada border raises per-shipment trucking costs. Brown (2012) estimates that shipping by truck from Canada to the U.S. costs 18–31% more than a comparable domestic shipment; Brown (2015) documents that the premium rose further after 9/11 with tightened customs and security requirements. Table 11 summarises the four channels through which the premium arises.

Channel	Mechanism	Source
Customs & documentation	Every commercial crossing requires Canada Border Services Agency (CBSA) clearance with Advance Commercial Information (ACI/eManifest) one hour before arrival and U.S. Customs and Border Protection (CBP) clearance via Automated Commercial Environment (ACE); bilateral commercial invoices, bills of lading, and Canada–United States–Mexico Agreement (CUSMA) certificates of origin. Average crossing time 26.8 minutes (95th pctile >70 min).	FHWA 2003; CBSA; CBP
Cabotage	Foreign carriers prohibited from domestic point-to-point hauling. A Canadian carrier delivering to a U.S. destination cannot pick up a domestic backhaul, forcing an empty return or wait for an international load; symmetric for U.S. carriers in Canada.	FMCSA; OBAC; CTA
Hours-of-service asymmetry	Canada allows 13 driving hours/day with 8 consecutive off-duty; U.S. allows 11/10. Cross-border drivers comply with the more restrictive U.S. rules, cutting daily driving capacity by ∼15%.	49 CFR 395; SOR/2005-313
Weight/dimension differences	The Canadian Interprovincial Memorandum of Understanding (MOU) on Vehicle Weights and Dimensions permits standard 5-axle tractor-semitrailer at ∼137,800 lbs in Canada; carrier must reduce payload to U.S. 80,000-lb Interstate limit at the border. Several provinces permit LCVs on designated highways that most U.S. border states prohibit.	CCMT MOU; FHWA

Table 11: Channels of the U.S.–Canada border premium.

C.4 Iceberg Cost Shocks

For three of the four counterfactuals, the figures below display the changes in iceberg costs by market type and origin. For the U.S.–Canada border closure, international markets

are removed entirely ($c_{ni} \to \infty$), so a corresponding figure is not informative.

Figure 2: Impact of Removing IHS on Iceberg Costs

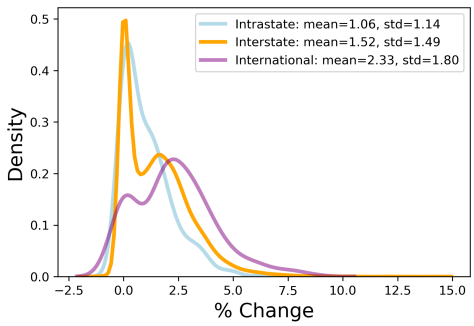

(a) By Market Type

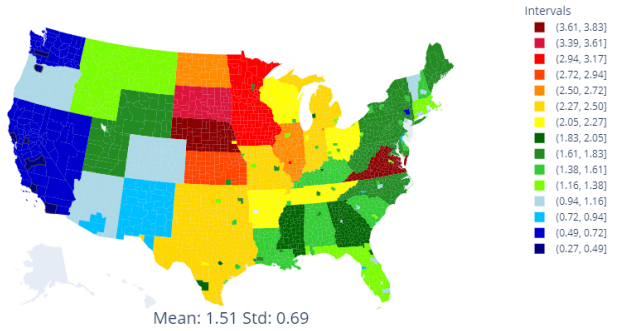

(b) By Origin

Note: (a) plots the distribution of percentage changes in iceberg trade costs across all (n, i) pairs, excluding Canada-to-Canada, by market type. (b) shows the percentage change in average iceberg trade costs for U.S. regions, $N^{-1} \sum_n \triangle \tau_{ni}$, for each origin i. Stronger increases are highlighted in red; weaker increases appear in blue.

Figure 3: Impact of Harmonization on Iceberg Costs

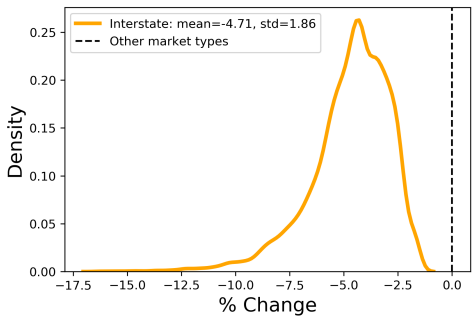

(a) By Market Type

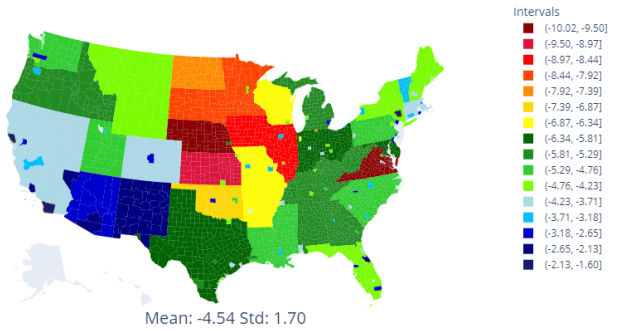

(b) By Origin

Note: (a) plots the distribution of percentage changes in iceberg trade costs across all (n, i) pairs, excluding Canada-to-Canada, by market type. (b) shows the percentage change in average iceberg trade costs for U.S. regions, $N^{-1} \sum_n \triangle \tau_{ni}$, for each origin i. Stronger decreases are highlighted in red; weaker decreases appear in blue.

Figure 4: Impact of Autonomous Trucks on Iceberg Cost

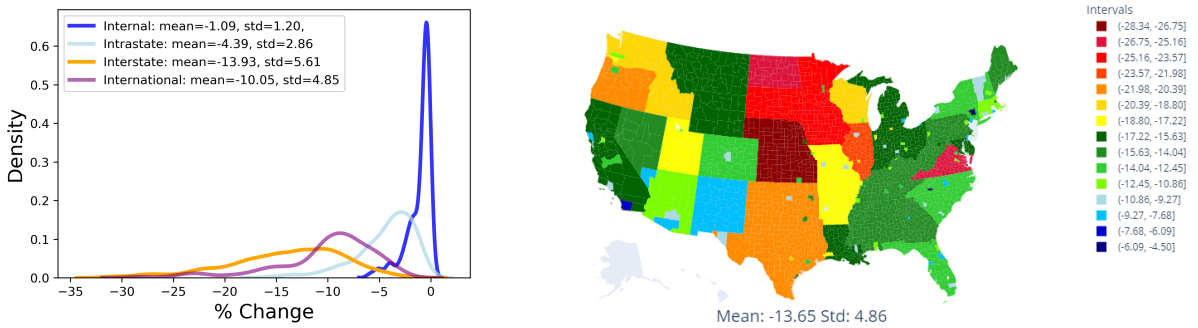

(a) By Market Type (b) By Origin

Note: (a) plots the distribution of percentage changes in iceberg trade costs across all (n, i) pairs, excluding Canada-to-Canada, by market type. (b) shows the percentage change in average iceberg trade costs for U.S. regions, $N^{-1}\sum_n \triangle\tau_{ni}$, for each origin i. Stronger decreases are highlighted in red; weaker decreases appear in blue.

C.5 Supply and Demand Shifters

Table 12 decomposes the supply and demand shifters at the medoid market for each market type and experiment. Across all four experiments, the supply shifter Δk_i and the expenditure-share shifter $\Delta \sum_j \alpha^j \pi_{ni}^j$ exceed the relative wage and destination-population shifters; the latter remain non-negligible in larger experiments (up to 3% for both relative wages and destination population in the autonomous-trucks experiment, and up to 4% for relative wages in the interstate-regulation harmonization experiment). Panel (c) of Figures 5–8 plots $\Delta k_i/k_i$ against the full demand bracket from (18); this table makes the per-component contribution explicit.

Table 12: Supply and Demand Shifters at Medoid Routes (% changes, baseline model)

		Shifters				Equilibrium	
Experiment	Market type	Δk_i	$\Delta \frac{w_n}{w_i}$	ΔL_n	$\Delta \sum_j \alpha^j \pi^j_{ni}$	$\Delta \tau_{ni}/\tau_{ni}$	Δk_{ni}
IHS elimination	Internal	−1.58	0.00	−0.19	10.08	0.47	9.36
	Intrastate	−2.58	−0.28	−0.34	3.79	1.07	2.05
	Interstate	−1.61	−0.26	−0.37	0.57	1.58	−1.62
	International	−1.58	−0.61	0.00	−1.61	2.48	−4.58
	CA Internal	−2.19	0.00	0.00	15.89	0.34	15.50
Interstate-regulation harmonization	Internal	4.47	0.00	0.45	−22.55	−1.22	−21.24
	Intrastate	4.10	4.30	2.79	−23.34	−0.94	−17.03
	Interstate	0.01	0.45	0.60	1.43	−5.11	8.03
	International	2.94	−2.29	0.00	−0.72	−0.15	−2.86
	CA Internal	−0.14	0.00	0.00	11.42	0.22	11.18
Border closure	Internal	2.12	0.00	0.49	25.53	0.78	25.17
	Intrastate	1.33	0.71	0.42	12.88	0.41	13.69
	Interstate	0.67	−2.15	−2.29	12.72	0.20	7.55
	CA Internal	−10.69	0.00	0.00	1,018.56	5.05	964.81
Autonomous trucks	Internal	17.17	0.00	1.41	−46.88	−4.36	−43.68
	Intrastate	17.28	2.58	3.01	−33.77	−5.87	−25.65
	Interstate	9.23	2.28	1.46	11.36	−14.97	35.90
	International	7.42	2.81	1.41	0.60	−10.37	17.02
	CA Internal	7.42	0.00	0.00	−10.01	−8.17	−2.00

Note: Each cell reports the exact ratio-based percentage change at the medoid route for the indicated market type. The medoid is the origin-destination pair that minimizes the sum of normalized Euclidean distances to all other pairs in its market type, computed in $(\Delta k_{ni}, \Delta \tau_{ni}/\tau_{ni})$ space—matching the medoid diamonds in panels (a) and (b) of Figures 5–8. Shifters correspond to equation (18): Δk_i is the supply shifter (change in total trucks from origin i); $\Delta(w_n/w_i)$ is the relative wage; ΔL_n is the destination population; $\Delta \sum_j \alpha^j \pi^j_{ni}$ is the expenditure-share shifter, computed from the identity $\sum_j \alpha^j \pi^j_{ni} = \alpha\, X_{ni}/(w_n L_n)$ (so its percentage change equals $X_{ni,\text{hat}}/(w_{n,\text{hat}} L_{n,\text{hat}}) - 1$). For the CA Internal row this composite has a small baseline ($\sum_j \alpha^j_{\text{CA}} \pi^j_{nn,0} \approx 0.014$) and a theoretical upper bound when $\pi^j_{nn} \to 1$ of $\sum_j \alpha^j_{\text{CA}} \approx 0.157$; the +1,018.56% figure in the border-closure row approaches this bound as Canadian imports from the U.S. are eliminated. The last two columns report equilibrium outcomes: $\Delta \tau_{ni}/\tau_{ni}$ is the change in the iceberg cost $\tau_{ni} \equiv \varphi_i + t_{ni}/w_i$; Δk_{ni} is the change in truck volume. The shifters and equilibrium outcomes satisfy eq. (18) at each medoid. International routes are excluded from the border closure experiment because $c_{ni} \to \infty$ on those routes.

C.6 Spatial Distribution of Real Income Effects

For each U.S. origin we report the baseline real-income percentage change and the amplification ratio (baseline / Iceberg Limit). The figures below show the spatial distribution; the prose summarizes each distribution by its median and full range across the 128 U.S. origins.

Eliminating the Interstate Highway System. Baseline U.S. real income falls at every origin: median −0.34%, range [−0.97%, −0.02%], with the Northeast and Midwest most affected. The amplification ratio has median 1.25 and ranges from 0.66 to 2.22 across origins.

Figure 5: Impact on Real Wage (%)

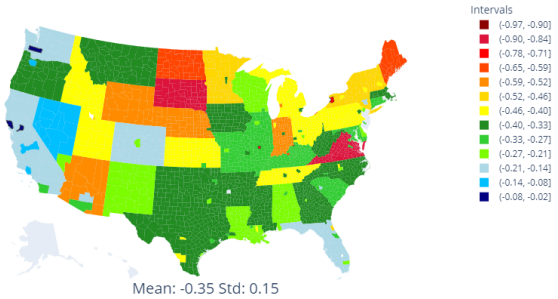

Note: The figure illustrates percentage changes in the real wage (relative to the price of tradable and non-tradable goods) in the baseline model. Stronger decreases are highlighted in red; weaker decreases appear in blue.

Figure 6: Amplification Effects on Real Wage

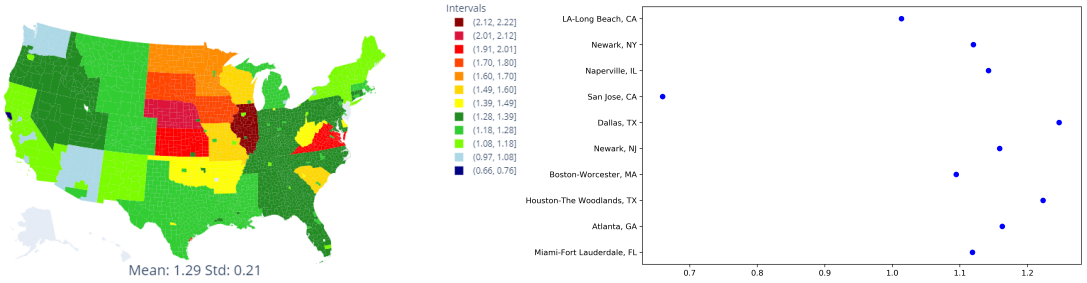

(a) Ratio by Geography in U.S. (b) Ratio by Top 10 Cities in U.S.

Note: (a) maps the amplification ratio of percentage changes in the real wage (relative to the price of tradable and non-tradable goods) between the baseline model and the Iceberg Limit, $d\log(w/P)^{\text{Baseline}}/d\log(w/P)^{\text{EK}}$, for each U.S. location. Stronger amplifications are highlighted in red; weaker amplifications appear in blue. (b) displays this ratio for the 10 largest U.S. cities by employment.

Harmonizing Interstate Trucking Regulations. Baseline U.S. real income rises at every origin: median +0.98%, range [+0.36%, +2.67%], with central states (NE, IA, MO) seeing the largest gains. The amplification ratio has median 1.26 and ranges from 1.05 to 2.33.

Figure 7: Impact on Real Wage in U.S.

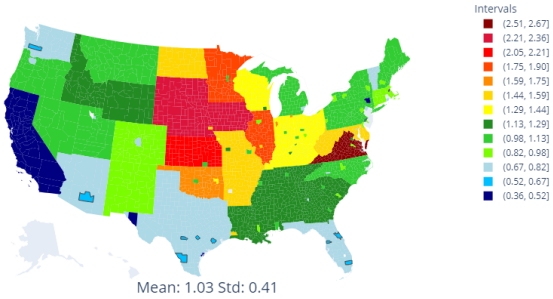

Note: The map displays percentage changes in the real wage (relative to the price of tradable and non-tradable goods) in the baseline model. Stronger increases are highlighted in red; weaker increases appear in blue.

Figure 8: Amplification Effects on Real Wage

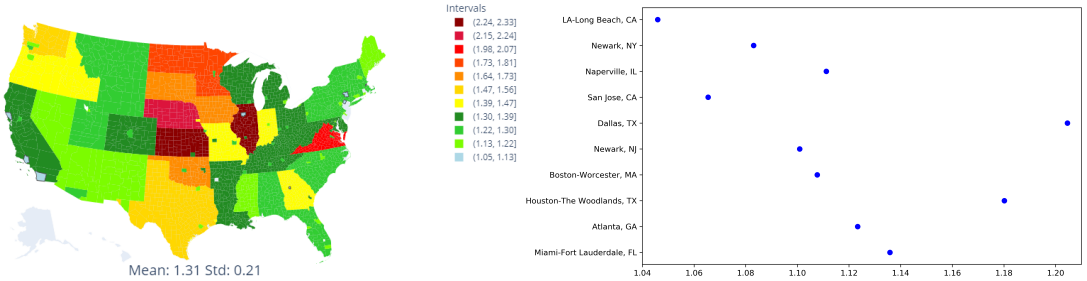

(a) Ratio by Geography in U.S. (b) Ratio by Top 10 Cities in U.S.

Note: (a) maps the amplification ratio of percentage changes in the real wage (relative to the price of tradable and non-tradable goods) between the baseline model and the Iceberg Limit, $d\log(w/P)^{\text{Baseline}}/d\log(w/P)^{\text{EK}}$, for each U.S. location. Stronger amplifications are highlighted in red; weaker amplifications appear in blue. (b) displays this ratio for the 10 largest U.S. cities by employment.

Shutting Down the U.S.–Canada Border. Baseline U.S. real income falls at every origin: median -0.43%, range $[-1.83\%, -0.13\%]$, concentrated in border regions of the Northeast and Great Lakes. The amplification ratio has median 1.08 and ranges from 0.92 to 17.55, with the upper tail driven by a small number of origins whose Iceberg Limit real-income change is near zero.

Figure 9: Changes in Real Wage (%)

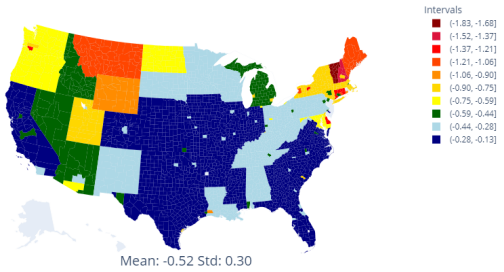

Note: The map displays percentage changes in the real wage (relative to the price of tradable and non-tradable goods). Stronger magnitudes are highlighted in red; weaker magnitudes appear in blue.

Figure 10: Amplification Effects of Transportation Markets on Real Wage

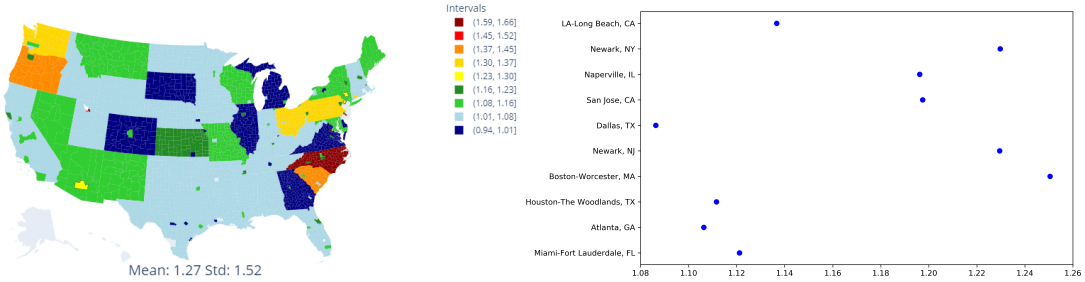

(a) Ratio by Geography in U.S. (b) Ratio by Top 10 Cities in U.S.

Note: (a) maps the amplification ratio of percentage changes in the real wage (relative to the price of tradable and non-tradable goods) between the baseline model and the Iceberg Limit, $d\log(w/P)^{\text{Baseline}}/d\log(w/P)^{\text{EK}}$, for each U.S. location. Stronger amplifications are highlighted in red; weaker amplifications appear in blue. (b) displays this ratio for the 10 largest U.S. cities by employment.

The Advent of Autonomous Trucks. Baseline U.S. real income rises at every origin: median +2.79%, range [+1.36%, +6.55%], with central states gaining the most. The amplification ratio has median 1.31 and ranges from 1.09 to 1.95.

Figure 11: Impact on Real Wage (%)

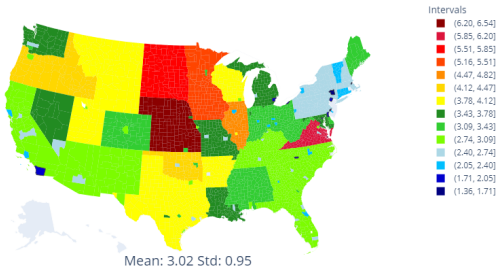

Note: The map displays percentage changes in the real wage (relative to the price of tradable and non-tradable goods) in the baseline model. Stronger magnitudes are highlighted in red; weaker magnitudes appear in blue.

Figure 12: Amplification Effects on Real Wage

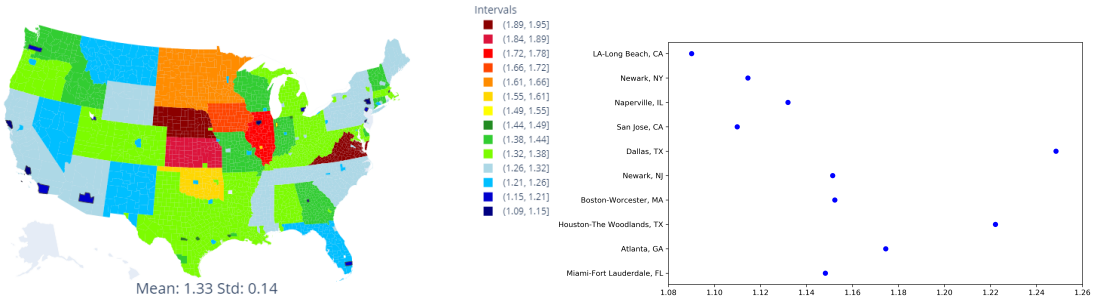

(a) Ratio by Geography in U.S.

(b) Ratio by Top 10 Cities in U.S.

Note: (a) maps the amplification ratio of percentage changes in the real wage (relative to the price of tradable and non-tradable goods) between the baseline model and the Iceberg Limit, $d\log(w/P)^{\text{Baseline}}/d\log(w/P)^{\text{EK}}$, for each U.S. location. Stronger amplifications are highlighted in red; weaker amplifications appear in blue. (b) displays this ratio for the 10 largest U.S. cities by employment.

References

Allen, T., Arkolakis, C., 2014. Trade and the topography of the spatial economy. The Quarterly Journal of Economics 129, 1085–1140.

Allen, T., Arkolakis, C., Li, X., 2024. On the equilibrium properties of spatial models. American Economic Review: Insights 6, 472–489.

Alvarez, F., Lucas, R.E., 2007. General equilibrium analysis of the Eaton–Kortum model of international trade. Journal of Monetary Economics 54, 1726–1768.

Anderson, T.W., Rubin, H., 1949. Estimation of the parameters of a single equation in a complete system of stochastic equations. Annals of Mathematical Statistics 20, 46–63.

Brown, W.M., 2012. Trucking across the border: The relative cost of cross-border and domestic trucking, 2004 to 2009. Economic Analysis Research Paper Series, No. 081 .

Brown, W.M., 2015. How much thicker is the Canada–U.S. border? The cost of crossing the border by truck in the pre- and post-9/11 eras. Economic Analysis Research Paper Series, No. 099 .

Caliendo, L., Parro, F., 2015. Estimates of the trade and welfare effects of NAFTA. The Review of Economic Studies 82, 1–44.

Caliendo, L., Parro, F., Rossi-Hansberg, E., Sarte, P.D., 2018. The impact of regional and sectoral productivity changes on the US economy. The Review of Economic Studies 85, 2042–2096.

Conley, T.G., 1999. GMM estimation with cross sectional dependence. Journal of Econometrics 92, 1–45.

Costinot, A., Donaldson, D., Komunjer, I., 2012. What goods do countries trade? A quantitative exploration of Ricardo's ideas. The Review of Economic Studies 79, 581–608.

Eaton, J., Kortum, S., 2002. Technology, geography, and trade. Econometrica 70, 1741–1779.

Finlay, K., Magnusson, L.M., Schaffer, M.E., 2014. WEAKIV: Stata module to perform weak-instrument-robust tests and confidence intervals for instrumental-variable (IV) estimation of linear, probit and tobit models. Statistical Software Components S457684, Boston College Department of Economics.

Head, K., Mayer, T., 2014. Gravity equations: Workhorse, toolkit, and cookbook, in: Handbook of International Economics. Elsevier. volume 4, pp. 131–195.

Keane, M.P., Neal, T., 2024. A practical guide to weak instruments. Annual Review of Economics 16, 185–212.

Mas-Colell, A., Whinston, M.D., Green, J.R., 1995. Microeconomic Theory. Oxford University Press, New York.

Redding, S.J., 2016. Goods trade, factor mobility and welfare. Journal of International Economics 101, 148–167.

Stock, J.H., Yogo, M., 2005. Testing for weak instruments in linear IV regression, in: Andrews, D.W.K., Stock, J.H. (Eds.), Identification and Inference for Econometric Models: Essays in Honor of Thomas Rothenberg. Cambridge University Press, pp. 80–108.